DETERMINING TRANSIT TIMES THROUGH HYPORHEIC ZONES USING PASSIVE TECHNIQUES IN RED BUTTE CANYON

by

Stewart Alan Gubler

A thesis submitted to the faculty of
The University of Utah
in partial fulfillment of the requirements for the degree of

Master of Science

in

Geology

Department of Geology and Geophysics

The University of Utah

December 2016

The University of Utah Graduate School

STATEMENT OF THESIS APPROVAL

The thesis of **Stewart Alan Gubler**

has been approved by the following supervisory committee members:

Douglas Kip Solomon	, Chair	**7/13/2016** Date Approved
Gabriel J. Bowen	, Member	**5/10/2016** Date Approved
Bernard Stolp	, Member	**5/10/2016** Date Approved

and by **John M. Bartley** , Chair/Dean of

the Department/College/School of **Geology and Geophysics**

and by David B. Kieda, Dean of The Graduate School.

ABSTRACT

Hyporheic flow has been identified as a major component of stream flow in Red Butte Canyon. While most hyporheic flow systems tend to have transit times of hours to days, previously conducted stream tracer tests suggest that, in Red Butte, these transit times are much longer. A stream survey of radon concentrations was used to identify specific areas of hyporheic discharge, including spring discharge from a tufa mound that is recharged from the stream approximately 200 m upslope. The hydraulic connection between the stream and the tufa spring was verified by performing an active bromide injection into the stream and monitoring for bromide concentrations in the spring. Two passive techniques, namely, variations of H and O isotope ratios and of noble gas concentrations, were evaluated as means of measuring hyporheic transit times. Peak concentrations of bromide in the tufa spring were observed approximately 18 days after a 24-h injection into the stream, with center of mass transit times of 34-48. However, substantial dispersion resulted in measurable bromide existing 17 weeks after injection. The stable isotope method used storm events with unique H and O isotopic values to reveal an approximately 16-day lag between the stream and the spring that discharges the hyporheic system. Dispersion resulted in significant flattening and spreading of the O and H peaks. However, with better resolution, the stable isotopes are the most promising passive technique. The noble gas method relies on the temperature dependence of the equilibrium solubility of atmospheric noble gases (e.g., Kr and Xe) combined with diurnal and seasonal temperature fluctuation

in the stream. However, a 27-h sampling event revealed that the spring had large variations in noble gas concentrations, even though its measured temperature was constant, which could be a result of some exposure to the air before the water is discharged. The noble gases in the spring showed apparent equilibration temperatures similar to the air temperature but lagged by about 13 h. With air temperature appearing to affect the solubility of the gases, and due to the size of the data population, conclusive results from the noble gases could not be determined.

TABLE OF CONTENTS

Appendices

LIST OF TABLES

Tables

LIST OF FIGURES

Figures

ACKNOWLEDGEMENTS

I would like to first and foremost thank my advisor Dr. Kip Solomon for the idea behind this research, as well as his full support, encouragement, and expansive knowledge on so many topics. None of this would have been possible without him. I would also like to thank Bernard Stolp for all of his help, especially in the winter, getting up Red Butte in the snow, showing me around the canyon, and helping collect samples. Wil Mace was a huge help, from help in the field collecting samples, to the lab where he taught me how to process and analyze the samples, as well as his friendship and constant encouragement. Cedar Coleman deserves a huge thank you as he helped so much, especially when lots of equipment was involved. He helped bring and set up equipment, take down equipment, and even camped to collect samples throughout the night. I would like to thank the many undergraduates and friends that came to help collect samples, especially Olivia Watkins and Brian Pfaff. Jennifer Georgek, who despite working on her own thesis, took time to help me in the field and provided great feedback on ideas. I would also like to thank the countless others who helped with analyzing samples: Diego Fernandez, Chris Anderson, Alan Rigby, Gabe Bowen and the SIRFIR lab, Chris Tingey, and many others. I also would not be where I am today without the support of my family and especially my wife. Their encouragement and support over the years has allowed me to get to this point.

1 INTRODUCTION

1.1 Background and hydrologic setting of Red Butte Canyon

Red Butte Canyon, located immediately east of the University of Utah in Salt Lake County, has been set aside as a research natural area since the 1960s. As such, it has experienced very few impacts or changes from the nearby population, making it an ideal location for studying ecosystems and hydrology. The drainage basin is characterized by a narrow canyon bottom with heavily vegetated, steep hillsides.

Red Butte stream starts at several springs in Knowltons fork, then gains and loses through many stretches down to its confluence with Parley's fork. The flow of the stream increases due to Parley's fork tributary, then flows into a reservoir before flowing into the urban environment of Salt Lake City. A U.S. Geological Survey gauging station located just above the reservoir has operated since 1963. Baseflow is relatively stable from year to year with an estimated average of 3,740 L/min. Peak flows vary strongly from year to year. In 2013, innovative Urban Transitions and Aridregion Hydro-sustainability (iUTAH) installed a gauge station in Knowltons Fork that measures the stream gage-height and temperature. Red Butte Canyon has a runoff ratio of about 20%, meaning 20% of the precipitation that falls on the watershed makes it to the gauge above the reservoir (Hely et al., 1971). Previous bromide injection tests in Red Butte Canyon have identified hyporheic flow as a dominant component of stream flow (Bencala et al., 2011; Stolp, 2014).

1.2 Hyporheic flows in Red Butte Creek

Hyporheic flow is of interest to many fields: hydrology, biogeochemistry, biology, and ecology (Gooseff, 2016). Hyporheic flows can be conceptualized as transient storage zones; water and solutes are temporarily stored in these zones leading to transport times that are significantly longer than the average surface water velocity (Bencala and Walters, 1983). Water that enters the hyporheic zone provides organic matter as well as dissolved oxygen to organisms that live within the zone (Boulton et al., 1998). These organisms, in turn, provide nutrients that then reenter the stream system. Hyporheic flow occurs as stream water enters the subsurface, typically because of topographic barriers, flows underground and travels either vertically beneath the stream or horizontally between meanders, and then reenters the stream farther downstream (Figure 1) (Gooseff, 2010). These discharge locations can appear as springs or discharge directly into the stream, leading to the idea that new groundwater is entering the stream. However, previous studies in the canyon have observed that the discharge near the top of the canyon is essentially the same (ignoring contributions from tributary streams) as just above the reservoir, nearly 5 km away (Bencala et al., 2011). This indicates that there is minimal new groundwater entering the stream.

Hyporheic flows are generally very shallow, ranging from centimeters to meters, and have transit times ranging from hours to a few days (Gooseff et al., 2006). However, results of a tracer test conducted in 2003 indicate that hyporheic flows in Red Butte have potential transit times of several weeks to months (Stolp, 2014). Approximate locations of hyporheic zones within the upper reaches of the canyon are shown on Figure 2.

1.3 Using radon to identify hyporheic zones

In order to locate areas where groundwater and longer hyporheic flow paths discharge, radon (^{222}Rn) was used. Radon is produced naturally in the subsurface through the decay of uranium isotopes and has a half-life of 3.8 days. Water travelling through the ground (aquifer and/or hyporheic zone) accumulates radon, as a dissolved gas, from sediments. When this water discharges, it mixes with the stream and starts exchanging with the atmosphere, but can be traced for a few 10s of meters (Cook et al., 2006). Thus, high concentrations of radon in the stream indicate approximate locations of the outflow of the hyporheic flow paths.

1.4 O and H isotopes as tracers

Both the oxygen and hydrogen atoms of the water molecule have stable isotopes that are used as tracers for water. The most common isotopes are ^{18}O and ^{2}H (abbreviated as D) and expressed in comparison to an internationally accepted standard sample of ocean water called Standard Mean Ocean Water (SMOW) (Mazor, 1997). When evaporation of water occurs, the vapor is depleted in the heavy isotopes, giving it negative δD and $\delta^{18}O$ values, whereas the liquid remaining is depleted in the light isotopes and has positive δD and $\delta^{18}O$ values (Gat, 1996). When precipitation falls and enters the ground, the signal from δD and $\delta^{18}O$ for individual storms or winter/summer seasons becomes dampened and shortened as it travels through the subsurface but can still be traced (Figure 3) (McGuire and McDonnell, 2006). Values of δD and $\delta^{18}O$ in precipitation vary in parallel, in response to factors such as temperature, amount of rainfall, distance inland from the coast, latitude, and altitude (Mazor, 1997).

Temperature plays a major role in determining the δD and $\delta^{18}O$ values of precipitation as changes in the temperature affect the isotopic fractionation of water. (Dansgaard, 1964). The temperature at which water is evaporated determines the initial composition of atmospheric water. As water vapor (cloud mass) moves, cools and starts condensing, the temperature at which it condenses to precipitation determines the composition of the initial precipitation, which will change as more of the initial cloud mass is removed (Mazor, 1997). Table 1 shows fractionation factors for both D and ^{18}O at various temperatures. Since δD and $\delta^{18}O$ are affected by temperature, their values also vary cyclically with the seasons. With warmer temperatures, meteoric water is more enriched in the heavy isotopes and, at colder temperatures, meteoric water is more depleted in ^{18}O (Figure 4).

Another important factor for δD and $\delta^{18}O$ values is altitude. Increasing altitude generally means decreasing temperature. As Mazor (1997) states, "As clouds rise up the mountains, the heavy isotopes are [precipitated out first] and the residual precipitation gets isotopically lighter." Because δD and $\delta^{18}O$ values vary with altitude, δD and $\delta^{18}O$ can be used to trace the recharge elevation of ground waters.

Another component that affects δD and $\delta^{18}O$ is the distance from the coast, or the continental effect. As a cloud mass moves inland, it will become isotopically lighter as it precipitates out the heavier waters first. The farther away the cloud is from the coast, the lighter and more depleted the water becomes. This effect can be masked by the other effects described above, but can still be an effective tool for determining the water's origin (Mazor, 1997).

When δD and $\delta^{18}O$ values from around the world are plotted together, they delineate the global meteoric water line (GMWL). There are exceptions, as noted in Figure 5, for

areas with closed basins, where evaporation is a dominant process. However, the GMWL is valid for much of the world. Local meteoric water lines have been defined for many locations. The local lines parallel the GWML but are shifted above or below depending on humidity and temperature.

1.5 Noble gases as tracers

The noble gases Ne, Ar, Kr, and Xe have been used extensively in dating and thermometry of groundwater. These gases, when dissolved in water, provide a snapshot of the water temperature during groundwater recharge. The solubilities of Ar, Kr, and Xe are especially sensitive to changes in temperature, which makes them useful for determining recharge temperatures (Mazor, 1972; Aeschbach-Hertig and Solomon, 2013). These gases are partitioned between water and the atmosphere as a function of the pressure and temperature where the liquid and gas phases are in contact. When groundwater moves below the water table and becomes isolated from the atmosphere, the concentrations of noble gases do not change (Mazor, 1997). Thus, the hyporheic transit time (thought to be on the order of weeks to months in Red Butte Creek) could be evaluated based on the time variability of the noble gas concentrations caused by seasonal variability of stream temperature.

Within the context of evaluating transit times of hyporheic flow, the concentration of noble gases in a stream that is in contact with the atmosphere will vary with stream temperature. In concept, hyporheic flow that becomes isolated from the atmosphere would retain the noble gas recharge temperature of the stream at the time when the hyporheic flow became isolated from the stream and atmosphere. Thus, the stream temperature changes as

reflected in noble gas concentrations in the hyporheic flow (e.g., from winter to spring) would lag at the discharge location. This concept is illustrated in Figure 6, which was generated by numerically equilibrating the stream water with the atmosphere at given (time varying) temperatures, transporting this water through the subsurface using the advection-dispersion equation, and converting the noble gas concentrations into an apparent recharge temperature. The lag between the stream and hyporheic discharge noble gas temperature then becomes a measure of the subsurface transit time of the hyporheic flow. This is only possible for systems where hyporheic flows have transport times on the order of weeks and months. Most hyporheic flows have average transit times on the order of hours.

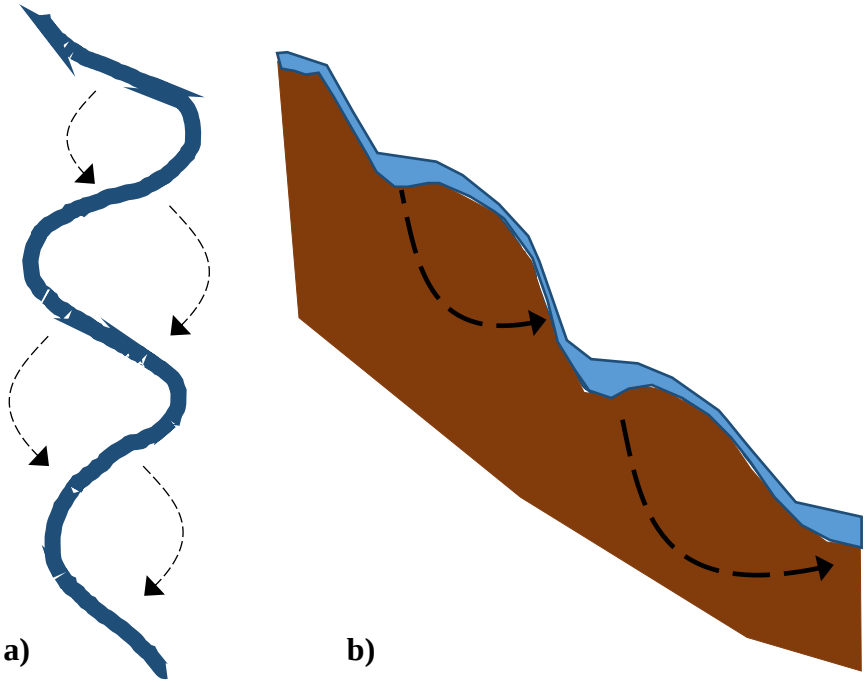

Figure 1. Conceptual models of hyporheic zones. a) Plan view of a stream where hyporheic flow occurs laterally. b) Cross section view of a stream where hyporheic flow occurs vertically. This most often occurs in streams with pools and riffles.

Figure 2. Map of study area. Notable landmarks are marked on the map. The orange star represents the site of the bromide injection and the highest sampling point. The yellow stars represent springs that are of particular interest. The blue star at Brush Basin represents where the stream is gaining flow, but not necessarily new ground water.

Table 1. D and ^{18}O isotope fractionation factors with varying temperatures (Dansgaard, 1964).

$t°C$	α_D	α_{18}
40	1.060	1.0074
20	1.079	1.0091
0	1.106	1.0111
-10	1.123	1.0123

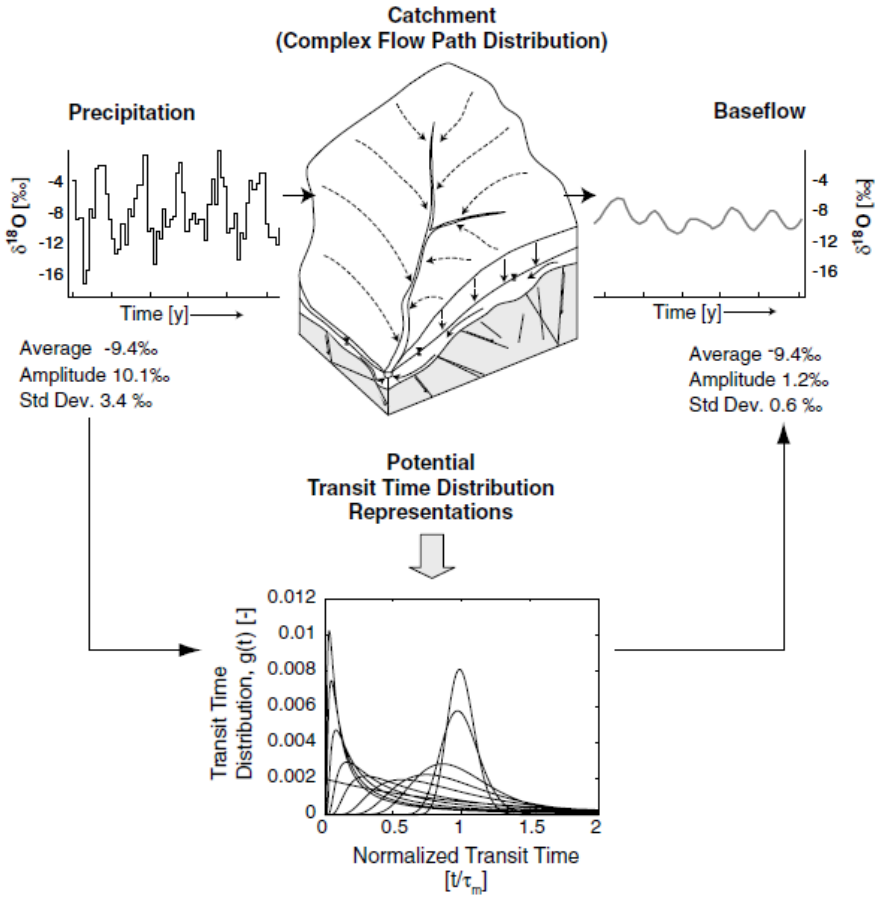

Figure 3. Conceptual diagram showing how temporal variation of $\delta^{18}O$ in precipitation is dampened and lagged due to transport. As precipitation falls over a catchment, the temporal tracers are transported through various flow paths until they reach the stream. As the tracers travel, the signal becomes dampened and lagged in comparison to the input signal due to dispersion and variations in the length of transport pathways within the catchment. Reprinted from Journal of Hydrology, Vol 330, McGuire and McDonnell, A Review and Evaluation of Catchment Transit Time Modeling, Pages 543-563, Copyright (2006), with permission from Elsevier.

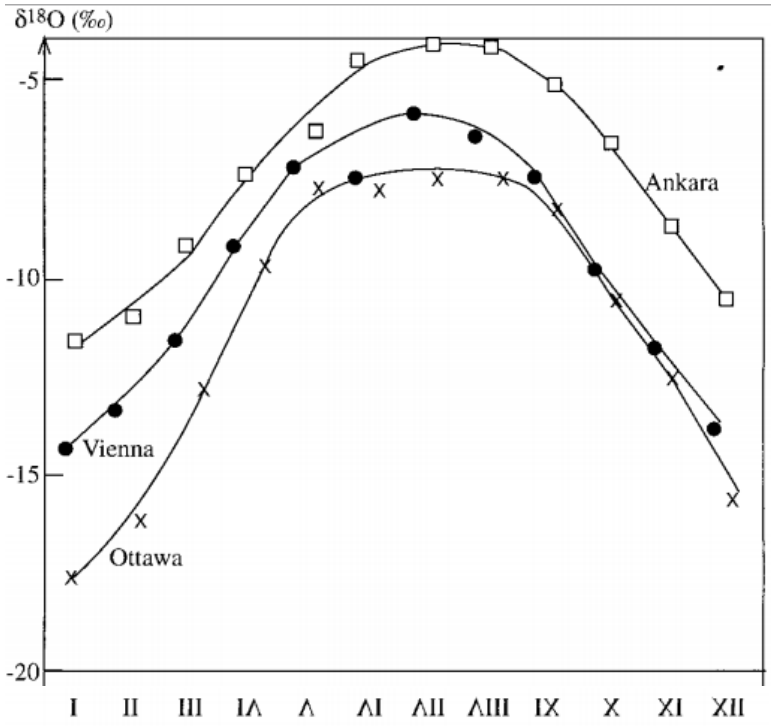

Figure 4. Variations in $\delta^{18}O$ over 1 year at 3 different locations. It is clear that during the summer months, with warmer temperatures, meteoric water becomes more enriched in the heavy O isotope, and then becomes more depleted during the winter months. Figure used from Gat (1996), Oxygen and Hydrogen Isotopes in the Hydrologic Cycle.

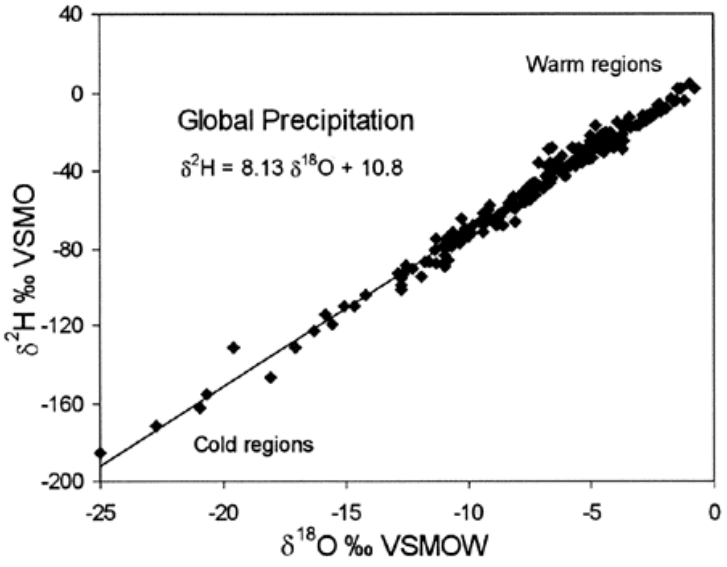

Figure 5. Plot of δD vs $\delta^{18}O$ of waters from around the globe. Despite a wide range in values, all, except for closed basins, plot on a straight line. This is known as the Global Meteoric Water Line (SAHRA - Isotopes & Hydrology, 2005).

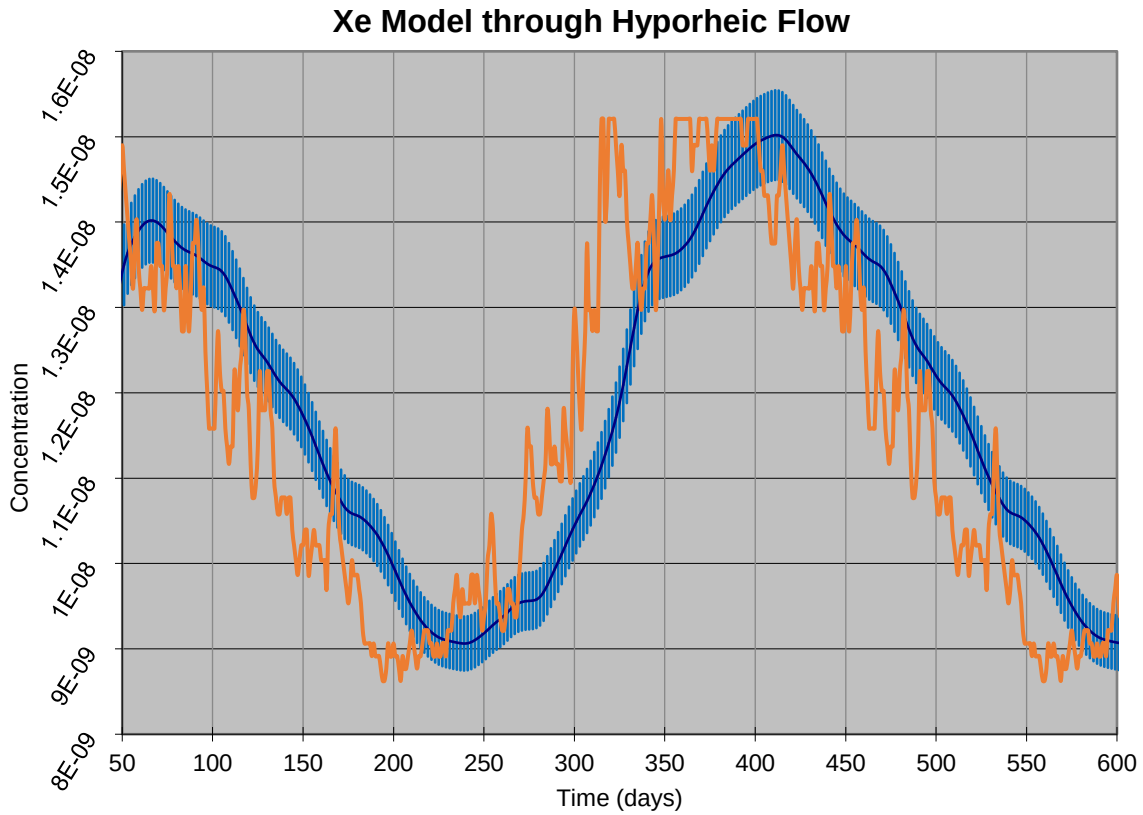

Figure 6. Xenon gas model through hyporheic flow. The orange line represents the theoretical equilibrium Xe concentration in stream water at the recorded stream temperature over two years. The dark blue line represents the Xe concentration after having been isolated from the stream and atmosphere and discharging from the spring. The blue lines are error bars of 3.5%. The model was created by solving the advection dispersion equation using a longitudinal dispersivity of 30 m and a velocity of 6.67 m/day. The model predicts that the concentration of Xe at the spring will lag the concentration of Xe in the stream by approximately 30 days.

2 METHODS

2.1 Using radon to identify hyporheic zones

Radon in Red Butte stream was measured by collecting 250 mL samples in glass bottles approximately every 100-500 m over a 4,900 m long reach that starts in Knowltons fork and ends at the U.S. Geological Survey gaging station (Figure 2). The bottles were rinsed 3 times with stream water before a sample was collected. The samples were then tested for radon using a Durridge RAD7 solid-state alpha detector. Due to the 3.8-day half-life of radon, samples were processed within 1 to 2 days after collection. The RAD7 has a detection limit of 0.5 pCi/L with an uncertainty of ± 5%. Based on results of the initial survey, more focused sampling was done within 3 sub reaches, located between Knowltons Fork and Brush Basin, to better determine discharge locations.

2.2 Bromide injection test

To characterize the discharge identified by the radon survey, a bromide injection test was conducted in November 2014. The objective was to evaluate the transit time and verify any hydraulic connection between the stream and the identified discharge locations. The timing for the injection test was chosen as this would be when the stream was at base flow with no evapotranspiration of stream water by riparian vegetation, and no input from early winter snowfall. Sodium bromide was chosen as a tracer because it is nonreactive and does not sorb to the sediment (Davis et al., 1998). A target stream concentration of 15 mg/L was

selected, which is approximately 100 times the detection limit for bromide (0.1 mg/L) and still well below the concentration that is potentially hazardous to most aquatic life (>500 mg/L) (Canton et al., 1983). With a measured stream discharge of 28 L/s, a Br injectate with a concentration of approximately 260,000 mg/L was injected into the stream for 26 h at an average injection rate of 100 mL/min (Figure 7). The injection site was the same as for the tracer test described in (Bencala et al., 2011)) and is located 200 m upstream from the tufa spring identified in the radon survey as a discharge location to Red Butte Creek.

The injection began at 8:20 am on November 11, 2014. During the injection, the stream was sampled roughly every hour during daylight hours. While there were variations in injection rate that make it difficult to estimate the stream concentration at any given time (see Appendix B), the total mass of bromide injected over 26 h is known to within 5%.

ISCO autosamplers were installed at the tufa spring and the lower spring to ensure samples could be collected every 6 h for the first 7 days. The ISCO samplers were originally covered with tarps to help insulate them from the cold. However, the ISCOs did freeze up a few times during the first week. To better insulate the ISCOs and prevent them from freezing, heating tape and insulation were applied to the inlet tubes. The heating tape and the ISCOs were powered by batteries and solar panels. All water samples in association with the Br injection test were filtered in the lab using polypropylene syringe filters with a pore size of 0.45 µm before being analyzed on a Metrohm 883 Basic Ion Chromatograph Plus using a Metrosep A Supp 5 – 150/4.0 column.

After one week with all spring water samples below detection, the sampling interval was increased to 12 h, and after two weeks it was increased to once a day. The rationale for changing the sampling interval is that the bromide peak will become more and more

spread out in the subsurface with time, due to dispersion. The peak bromide is an important parameter as it is one measure of the mean transit time through the hyporheic system. Another important transit time parameter is the center of mass. Within the system, there will be some pathways that transmit the water more rapidly and others that transmit the water more slowly, but the average pathway transit time is determined from the center of mass of the recovery curve. Samples continued to be collected daily until no more bromide was detected in the water, which was approximately 15 weeks after the injection.

2.3 Stable isotopes

At the start of the field investigation, δD and $\delta^{18}O$ samples were collected roughly every two weeks. Once the hyporheic zones were identified and characterized, water samples were collected every week starting in the winter of 2014 and continuing until the fall of 2015. Samples were collected in 50 mL glass vials. The vials were rinsed a minimum of three times with spring/stream water before a sample was collected. The samples were analyzed by the Stable Isotope Ratio Facility for Environmental Research (SIRFER) on a Picarro cavity ringdown spectrometer.

The stable isotope method is a "natural" analog to the bromide injection test. The difference is that, instead of injecting bromide, storm events act as injection tests. Each storm has a unique isotopic identity that can be measured and traced. Ideally, the stream reaches the isotopic composition of the storm and enough of that composition enters the hyporheic system so as to be detected at a future time without being completely attenuated by dispersion. However, the stream, while having its own isotopic composition, will not completely reach the storm's composition, but will rather be a mixture of the storm and the

stream compositions.

2.4 Noble gases

Noble gas samples were collected starting in the spring of 2015. These were collected in 26" long copper tubes with clamps on both ends. To collect a sample, the copper tube was placed horizontally into the stream or spring with a syringe attached to enhance flow-through. Once the tube had been purged several times, the end submerged in water is clamped shut. To ensure that any gas exchange during flow-through was redissolved, water in the syringe was used to pressurize the tube while the downstream end was clamped shut. The contents of each tube were analyzed in the Noble Gas Lab at the University of Utah on a mass spectrometer (Solomon, 2007). The assumption made for the stream is that the noble gas concentrations of water entering the hyporheic zone were in equilibrium with the stream at the average stream temperature.

With the concentrations of noble gases measured, recharge temperatures can be calculated. When calculating recharge temperatures from noble gas concentrations, excess air needs to be accounted for. There are various models that seek to deal with excess air; however, the closed-system equilibration model (CE) is the model that was used. This model assumes that "solubility equilibrium is attained in a closed system of initially air-saturated water and a finite volume of entrapped air under a constant hydrostatic pressure" (Aeschbach-Hertig et al., 2000). The equation used to calculate recharge temperature is:

$$C_i(T, S, P, A_e, F) = C_i^*(T, S, P) + \frac{(1 - F)A_e z_i}{1 + F A_e z_i / C_i^*} \quad (1)$$

where $C_i^*(T, S, P)$ are the moist-air solubility equilibrium concentrations as a function of temperature, salinity, and atmospheric pressure, F is the fractionation parameter, A_e is the

initial amount of entrapped air per unit mass of water, and z_i are the volume fractions of individual gases in dry air.

Samples were collected in copper tubes every week throughout the spring and summer of 2015. Samples were generally collected near the same time of day each week. However, this was not always possible. Temperature probes were installed at several locations. To check the assumption that dissolved gas in the stream is in equilibrium with air temperature at the time it enters the hyporheic zone, a 28-h sampling event was planned for the end of October. Samples were collected every 4 h from the spring (which showed little temperature variation), and every 4 h from the stream, with samples collected every 2 h during the afternoon to catch the rapidly changing temperatures. Sampling began on October 27, 2015, at 8:00 am, and ended at 11:00 am on October 28, 2015.

Figure 7. Photos of the set up for the bromide injection test. The top photo shows the overall setup at the top of a small cascade. The bromide solution is injected into the top of the cascade which allows for rapid mixing with the stream. The lower left picture shows the tank and pump setup. The lower right shows a close up of the pump used. The pump was programmed to inject 100 mL/min. (Photos by Stewart Gubler)

3 RESULTS

3.1 Radon survey

The radon stream survey proved to be very useful in identifying the discharge locations of hyporheic flows. Radon identified three potential areas of subsurface inflow to the stream (Figure 8). Two of these areas have associated springs a few meters away from the stream channel which had not been identified previously. These springs provided the best sampling as they were isolated from the stream and there was no fear of contamination, either from injection tests or mixing of spring and stream water. The easternmost spring discharged from the base of a large tufa mound roughly 10 m from the stream. The second spring, approximately 300 m downstream of the first, discharged near the base of a hill about 5 m from the stream. The last location identified with radon was near Brush Basin. Here, the discharge occurred within the stream channel. The uppermost zone was chosen as the focus area for this study.

3.2 Bromide injection

Bromide concentrations in the stream during the injection are shown in Figure 9. While there were some issues with the pumping rate for the first several hours, the stream reached a peak Br^- concentration of 33.6 mg/L approximately 8 h after the injection began. Despite the early issues with the pump and pumping rate, the stream reached an average concentration of approximately 24 mg/L during the 30-h injection period.

Bromide concentrations from the tufa spring are shown as a function of time in Figure 10. The first 3 samples had measurable Br^- concentrations, but the next 19 samples were below detection. However, 8 days after the injection, detectable concentrations of Br- began occurring in the Tufa Spring and increased from 0.14 mg/L to a peak of 0.66 mg/L 18 days after the injection.

The bromide showed that a significant amount of the water discharging from the springs, especially the tufa spring, was derived from the stream. The first few samples were contaminated because they show measurable Br^- before the injection test occurred. It is possible that while mixing the NaBr solution, some spilled onto a shoe or hand that contaminated the spring.

The bromide test allowed for the detection of a range of mean transit times through the hyporheic system at the tufa spring. The mean transit time is calculated based off of the center of mass of the plume, which in a Gaussian curve is the same as the peak. However, in Red Butte, there is a significant tail, which means the peak and the center of mass are not the same, indicating a large range of transit times. Mean transit time can be used to calculate the storage of the hyporheic zone as it is a function of the volume of water stored divided by the flow, or discharge. The first traces of bromide appeared 8 days after the injection. However, the peak of the bromide did not occur until 18 days after the test was conducted. Traces of bromide were seen for about 15 weeks after the injection had finished, indicating significant dispersion occurs in the system. Calculating the center of mass of the entire bromide curve (including the long tail just above detection), a mean transit time of 48 days is obtained. If the tail is truncated on January 27, 2016, a mean transit time of 34 days is calculated. Thus, the estimated values of the mean transit time of the hyporheic

system range from 18 – 48 days.

Using the range of mean transit times and assuming that the spring maintains a discharge of 1.8 L/s, a storage volume of 2,799,360 – 7,464,960 L is calculated. Taking the average of those volumes, approximately 5,100 m^3 of water are stored which, combined with other downstream zones, help to maintain baseflow during the summer months and could buffer the stream during short-term droughts.

To evaluate if the range of volumes of water calculated could feasibly be stored in the hyporheic zone, I divide the amount of water by an assumed porosity of 20% to get a total volume. The tufa spring is roughly 200 m from the injection site, and this represents a maximum length of the hyporheic zone. The width of the hyporheic zone could be anything from a few meters to over 200 m (since the stream flows for over 200 m before the spring discharges in to it). If we assume a length of 200 m, a width of 200 m and solve for the depth, we get a depth between 0.35 – 0.93 m. Thus, the amount of water calculated to be stored in the hyporheic zone could easily fit within those parameters. If we go on to assume the width is narrower than 200, for example, 50 m, then the hyporheic zone would extend to a depth of 1.4 – 3.7 m. This is also a plausible depth for the hyporheic flow in Red Butte Canyon.

The bromide test also allowed for calculation of the amount of spring water that originated in the stream using a mass balance of bromide. A total of 39.8 kg of bromide was injected into the stream. The mass of bromide that discharged from the spring was calculated by taking the concentration in the samples multiplied by the discharge of the spring. The discharge, while not measured frequently, was assumed to remain constant at 1.8 L/s year round. The mass of bromide discharged from the spring was computed to be

4.2 kg, nearly 10% of the mass injected into the stream. Knowing that approximately 10% of the bromide appeared in the spring, and knowing the concentrations in the stream and spring, as well as the discharge at the spring, a few simple calculations can be made to assess the amount of groundwater discharging from the spring. First, a simple mass balance equation is used to solve for the discharge of the stream during the injection test:

$$Q_{pump} \times C_{injectant} = Q_{stream} \times C_{stream} \quad (2)$$

where Q is the discharge and C is the concentration of bromide. Solving for the discharge of the stream yields 15.83 L/s. Since 10.6% of the stream discharges from the spring, and knowing the spring has a discharge of 1.8 L/s, I compute that approximately 93% of the spring discharge is hyporheic flow. That leaves approximately 7%, or 0.13 L/s, for either groundwater or flow that entered the hyporheic zone above the injection site.

While the lower spring had a clear initial breakthrough curve, its observed concentrations were smaller than in the tufa spring and only marginally above the detection limit (Figure 11). Measurable bromide was detected 8 days after the injection. It appeared to peak 18 days later at 0.238 mg/L and then to decline slightly after 24 days. However, the measurements began increasing again, possibly due to bromide discharging from the tufa spring or a more complex flow path.

Data from the bromide test were used to develop a transport model. The model is based on the Ogata-Banks (Ogata and Banks, 1961) solution to the advection-dispersion equation. The advection-dispersion equation is:

$$D\frac{\partial^2 c}{\partial x^2} - v\frac{\partial c}{\partial t} = R\frac{\partial c}{\partial t}; \quad (3)$$

where R is the retardation factor, v is the advection term, and D is the dispersion term and can be rewritten as:

$$D = \alpha v; \quad (4)$$

where α is the longitudinal dispersivity and v is the average linear velocity. The model was calibrated to the bromide data (Figure 10) by adjusting the average linear velocity (v) and dispersivity (α). The simulation fits the first 30 days reasonably well, but does not predict the long tail in the observed concentrations. The calibrated dispersivity is 30 m, with a velocity of 0.28 m/h. An effective diffusion coefficient of 1.0E-10 m^2/h was used for these simulations.

While the model results do not have as large a tail as the observed data, they match the initial breakthrough and peak quite well. The observed tailing may be a result of dual (or multiple) porosity transport that is not included in the numerical model. Dual porosity transport is common in fractured porous media. Fluid flow will be fast through the fractures, diffusing solutes into the matrix due to concentration gradients. Once the solute has flushed through the fracture, it will start diffusing out of the matrix, causing a long tail in the solute breakthrough curve (Douglas and Arbogast, 1990; Haws et al., 2005; Zimmerman et al., 1992).

3.3 Stable isotopes

While sampling for stable isotopes began in early 2014, the best results came after the bromide test when the sampling interval was changed to weekly to increase resolution. A storm in late May showed a significant difference in the composition of the stream and spring. While it is difficult to see an offset from that storm, it is apparent that there is a difference between the stream and the spring compositions during storm events. During June, when there was very little precipitation, the stream and the spring compositions track

each other. One storm in particular provided the best results for measuring the lag between the stream and the spring. A storm on July 9 produced approximately 1.38 cm of rain with an isotopic composition of nearly -10 ‰. On July 16 when a sample was taken, there was a much smaller storm, producing only 0.09 cm of rain with a composition of approximately -6 ‰. The stream did show a peak on July 16 while the spring had a measured peak on August 1, 16 days after the stream (Figure 11). The spring response is within the range of Br injection-derived mean transit time estimates.

Results from the SIRFER lab have very small uncertainties, typically between 0.02-0.04 ‰. The largest uncertainty in the stable isotope data comes from the sampling frequency. With only sampling once a week, it is possible to miss the peak from a given storm event. However, from the data, it appears that the lag between the spring and the stream is approximately 16 days ± 7 days. With increased sampling frequency, for example, daily, especially immediately before, during, and immediately after a storm, more conclusive results from stable isotopes could be achieved.

3.4 Noble gases

Measurements of noble gas concentrations permitted apparent recharge temperatures to be calculated using the CE model. Table 2 shows differences between measured and theoretical concentrations of the gases as well as the sum of chi squared, which is the sum of the individual chi-squared values for each gas except nitrogen. Values of chi-square are calculated by subtracting the expected values from the observed, squaring the difference, and then dividing by the expected value. The smaller the chi-squared value, the better the fit. As can be seen from the sum of chi-squared values, the CE model fits the data quite

well. Noble gas concentrations from weekly sampling of the stream showed variations in apparent recharge temperatures that ranged from 2.7 to 12.4 Celsius (Figure 12). This was thought to be a result of collecting samples at different times of the day. That is why the 27-h long sampling event was planned. The results from the diurnal sampling revealed some interesting trends that were not expected (Figure 13).

First, while the stream had an average temperature of 6 ˚C with a standard deviation of 0.92 ˚C, the recharge temperatures calculated from the noble gases showed an average temperature of 4.3 ˚C with a standard deviation of 1.6 ˚C. During the sampling period, the air temperature varied from 10 ˚C to below -2 ˚C. Comparing the noble gas derived temperatures to stream temperatures, the noble gas temperatures were always in excess of the air-equilibrated dissolved-gas values (cooler theoretical noble gas stream water temperatures). When the air temperature was drastically colder than the stream temperature, the dissolved noble gas concentrations were closer to air temperature equilibrations than stream temperature equilibration values.

Another interesting phenomenon that was seen from the noble gases was from the spring. While the temperature of the spring water maintained an average temperature of 7.9 ˚C with a standard deviation of 0.04 ˚C during the event, the apparent recharge temperatures from the noble gases did not maintain a steady temperature. Instead, the recharge temperatures had an average value of 5.7 ˚C and a standard deviation of 1.3 ˚C. The apparent recharge temperatures from the spring had two peaks, despite the constant spring water temperature. The recharge temperatures were then compared to the air temperatures during the event. It was observed that the air temperature also had two peaks during the event. The air and the recharge temperature peaks appeared to be offset from

each other by roughly 13 h. Thus the air appears to have affected the noble gases in the spring.

When sampling at the spring, one can hear a bubbling sound as the water leaves the tufa mound. This suggests exposure to air inside the tufa where it cannot be directly observed. This complicates the noble gas results as we are no longer sampling the water right where it exits the ground, but rather sampling it after it has been exposed to the atmosphere. Therefore, it is difficult to determine a transit time for the hyporheic flow from the noble gases. The simultaneous sampling of stream water known to recharge the spring, and the spring water, show that for this simple recharge-discharge system there are fundamental questions that have not been answered. They include the questions of excess noble gas concentrations in stream water, and the apparent dispersion of the stream noble gas input function at the spring. The lack of fluctuations at the spring might be due to diurnal fluctuations (approximately 4 ˚C) that are approximately the same as the seasonal stream temperature fluctuations.

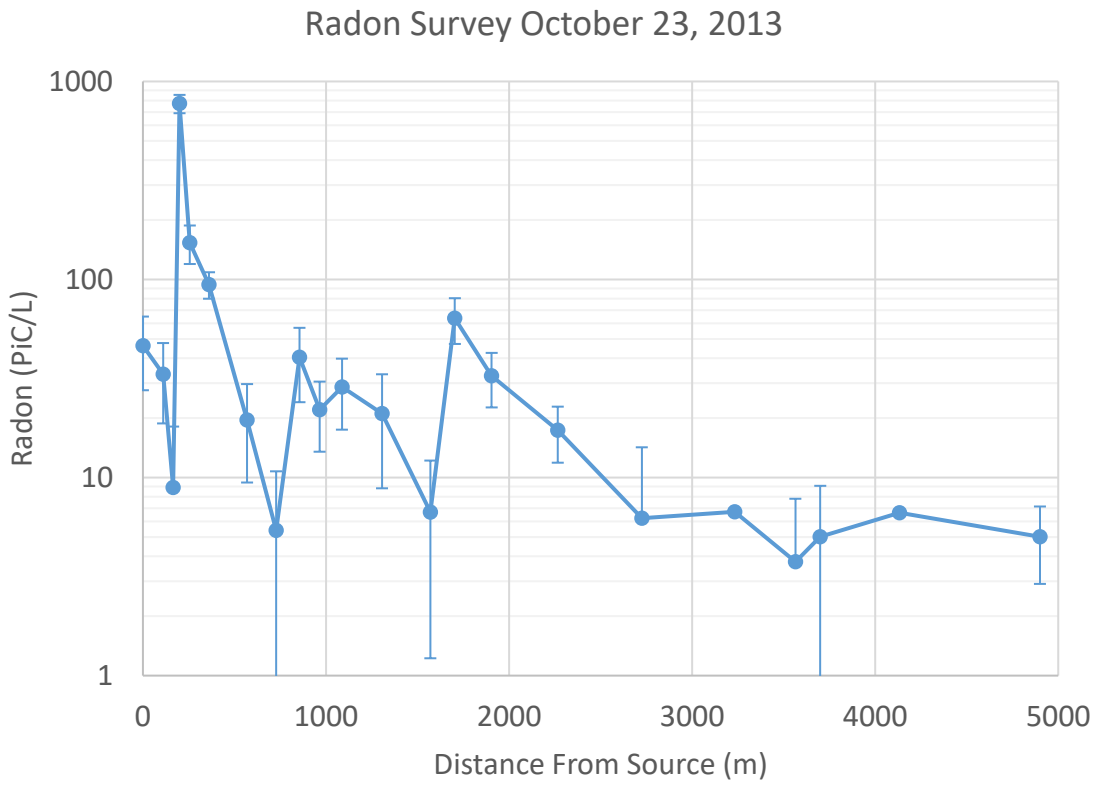

Figure 8. Results of the radon survey. Radon values are plotted on a logarithmic scale as a function of distance from the bromide injection site. Three spikes in radon indicated potential sites of hyporheic discharge. These occurred roughly 200 m, 800 m, and 1700 m from the site of injection. The first two spikes lead to the discovery of springs that were located just off of the stream channel.

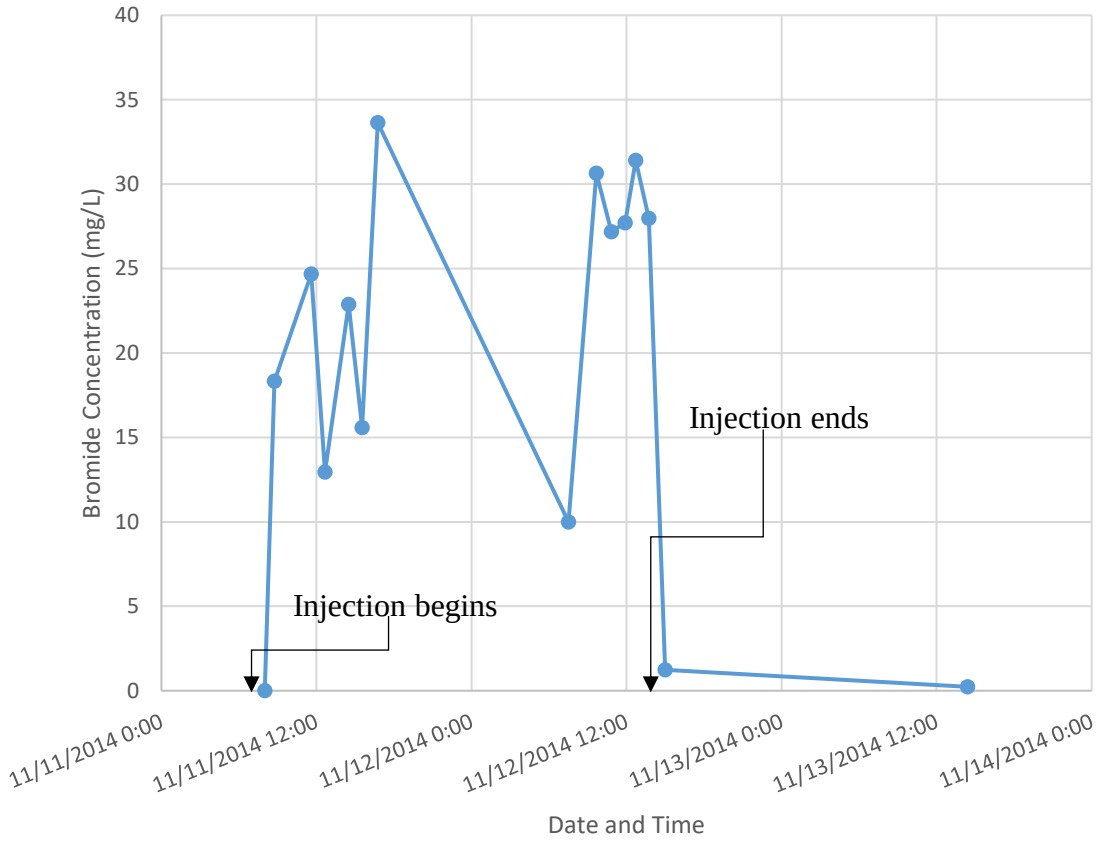

Figure 9. Bromide stream concentrations. Samples were taken roughly every hour from the stream 100 m below the injection site. The fluctuations are the result of issues with the pump. While a pumping rate of 100 mL/min was planned, there were issues with the pump controller that resulted in a fluctuating pump rate. During the first few hours, the pump would turn off after about an hour. This was eventually remedied. The pump rate slowed gradually throughout the night but was adjusted early in the morning. The stream peaked at nearly 35 mg/L and was completely flushed out within a day after injecting stopped.

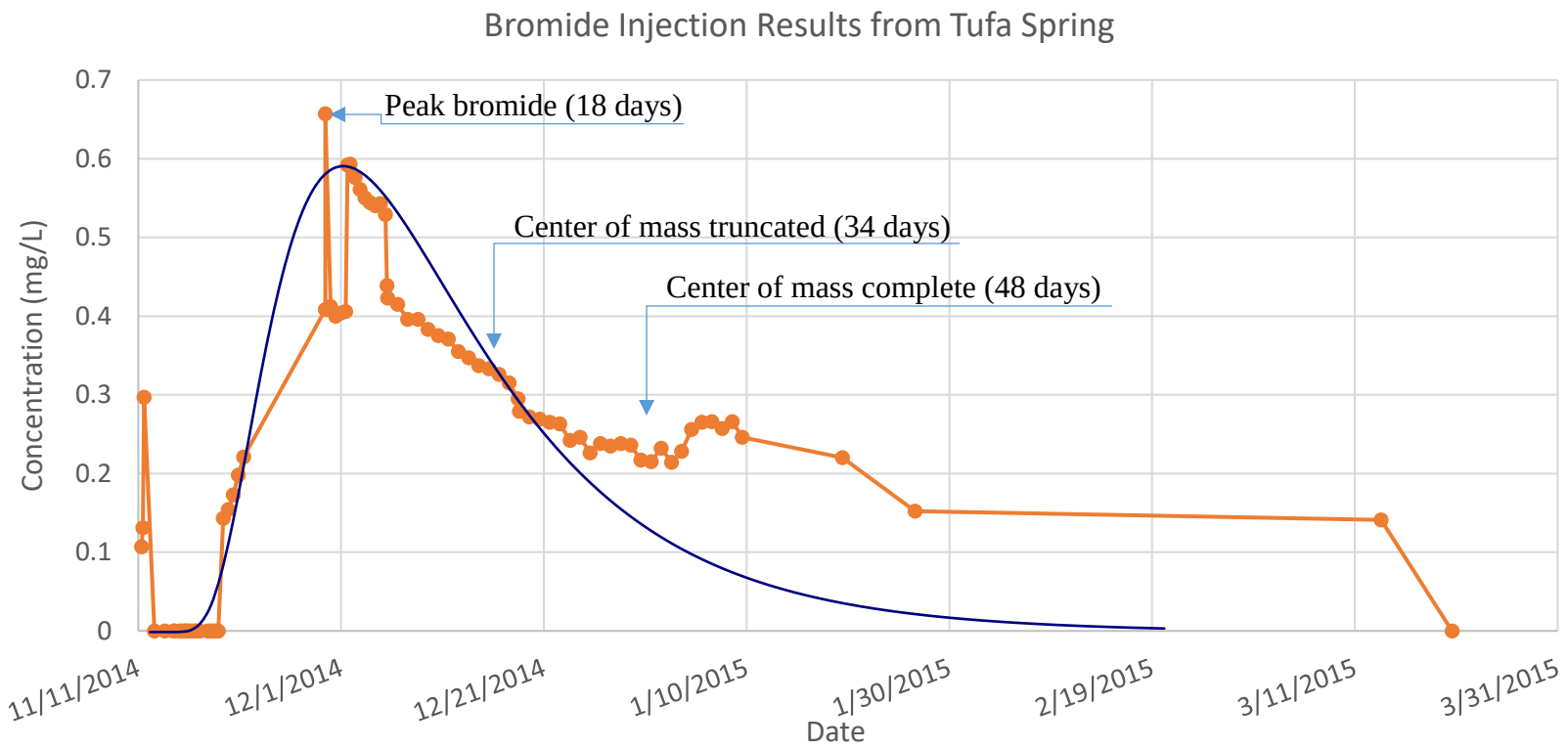

Figure 10. Results and model of the bromide injection test at the tufa spring. The orange line represents the collected data. Elevated concentrations in first 3 samples were likely the result of contamination. The first measurable traces of bromide occurred 8 days after the injection test. The peak, however, did not occur until approximately 18 days after the injection. After the peak, there was a steady decline in bromide. Bromide was still detected for about 15 weeks, indicating a large amount of dispersion occurring within the system. The center of mass for the entire curve gives a mean transit time of 48 days, while truncating the long limb gives a transit time of 34 days. The dark blue line is the model. While it does not capture the extent of the dispersion that occurred, it does accurately capture the initial breakthrough curve and the peak.

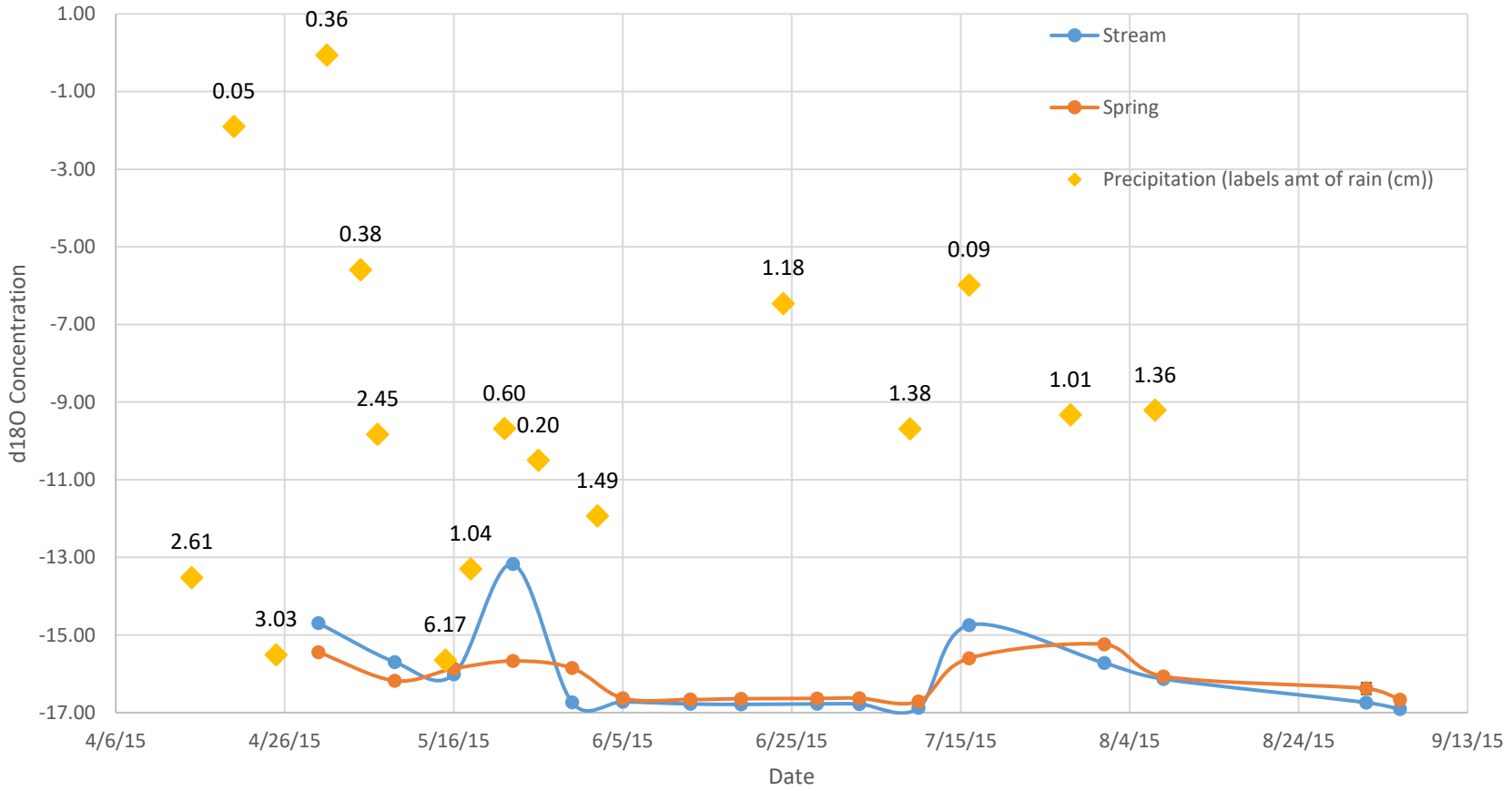

Figure 11. $\delta^{18}O$ results with precipitation events plotted. The blue line is the stream, orange is the spring, and yellow diamonds are storm events with the amount of rain labeled above each point. The individual storm events are hard to pick up from the spring. However, the best result is from the storm event in the middle of July. This storm dropped approximately 1.38 cm of ~-10 ‰ $\delta^{18}O$ on July 9. On July 16, there was a smaller storm event, but the stream still had a peak of about -15 ‰ $\delta^{18}O$. The spring didn't peak until roughly 16 days later on August 1st.

Table 2. Errors and Sum of Chi Squared Values for the Stream and Tufa Spring

Site	Date/Time	% Difference Between Measured and Theoretical						Sum
		Xe	N2	Ar	Ne	Kr	He4	χ^2
RB0	11/5/2014	-0.18%	28.%	1.7%	-3.1%	5.4%	-0.82%	1.5
RB0	4/18/2015	0.06%	27%	1.3%	-2.9%	9.1%	1.0%	1.2
RB0	4/25/2015	0.81%	-22%	0.37%	-3.4%	-0.69%	0.92%	1.4
RB0	4/30/2015	0.77%	27%	0.27%	-3.2%	7%	-1.7%	1.3
RB0	5/9/2015	2.4%	3.5%	0.47%	-9.6%	5.7%	-9.2%	13
RB0	5/15/2015 12:00	-2.3%	21%	5.6%	-3.1%	12%	-0.47%	4.9
RB0	5/23/2015 11:00	-0.07%	54%	2.0%	-3.9%	1.1%	-1.1%	2.3
RB0	5/30/2015 10:30	-2.3%	32%	5.2%	-2.6%	2.2%	-1.5%	4.1
RB0	6/5/2015 11:00	0.61%	34%	1.1%	-4.1%	0.48%	-0.16%	2.2
RB0	6/13/2015 8:00	2.7%	-3.1%	-1.8%	-1.8%	11%	0.08%	1.9
RB0	6/19/2015 11:00	0.20%	-21%	0.27%	-1.3%	6.1%	-0.57%	0.20
RB0	6/28/2015 8:30	3.2%	5.1%	-2%	-5.1%	7.8%	-0.88%	4.7
RB0	7/3/2015 9:00	8.5%	-14%	-7.7%	-3.4%	0.26%	0.44%	16
RB0	7/10/2015 17:30	-2.2%	41%	5.1%	-2.5%	13%	-1.6%	3.9
RB0	7/16/2015 17:00	-1.0%	-21%	3.1%	-2.9%	-1.5%	-0.37%	2.1
RB0	8/1/2015 10:00	0.16%	36%	1.0%	-2.7%	4.7%	-1.3%	0.98
RB0	8/8/2015 10:00	-0.09%	-8.3%	1.7%	-3.3%	2.9%	-1.1%	1.6
RB0	9/1/2015 15:00	2.3%	-13%	-1.6%	-3.6%	-0.43%	-0.59%	2.4
RB0	9/5/2015 9:30	0.80%	-19%	1.2%	-5.0%	6.9%	-0.08%	3.3
RB0	9/12/2015 7:40	2.6%	-18%	-2.1%	-3.3%	0.12%	-0.67%	2.5
RB0	9/19/2015 7:40	0.73%	-17%	0.53%	-3.4%	5.2%	-0.87%	1.5
RB0	9/27/2015 9:30	4.2%	-23%	-3.4%	-4.4%	0.44%	-1.7%	5.5
RB0	10/2/2015 7:30	2.2%	-30%	-1.7%	-2.9%	3.3%	-3.2%	1.8
RB0	10/9/2015 7:15	1.7%	-19%	-0.09%	-4.8%	-1.4%	-0.75%	3.1
RB0	10/15/2015 16:40	2.1%	-8.4%	-1.6%	-3.1%	-0.05%	-2.4%	1.9
RB0	10/27/2015 8:00	4.2%	-16%	-4.1%	-2.8%	1.6%	-1.8%	4.8
RB0	10/27/2015 12:00	1.4%	-21%	0.51%	-5.1%	2.1%	-1.9%	3.5
RB0	10/27/2015 14:00	5.6%	-3.8%	-2.9%	5.5%	5.5%	-1.0%	14
RB0	10/27/2015 16:00	4.2%	-25%	-1.5%	-8.2%	0.49%	-1.6%	11
RB0	10/27/2015 18:00	-0.21%	-17%	2.3%	-4.1%	2.0%	-2.2%	2.5

Table 2 cont.

Site	Date/Time	% Difference Between Measured and Theoretical						Sum
		Xe	N2	Ar	Ne	Kr	He4	χ^2
RB0	10/27/2015 20:00	-0.46%	-7.6%	2.4%	-3.4%	3.2%	-1.5%	2.0
RB0	10/28/2015 0:00	1.4%	-17%	-0.28%	-3.5%	4.1%	-1.6%	1.7
RB0	10/28/2015 4:00	2.4%	-5.3%	0.47%	-7.6%	-1.2%	-2.7%	8.1
RB0	10/28/2015 8:00	2.0%	-13%	-0.88%	-4.1%	4.4%	-1.4%	2.5
RB0	10/28/2015 11:00	4.0%	-24%	-4.6%	-1.1%	3.0%	-2.7%	4.4
Spring	11/5/2014	-0.89%	-19%	1.5%	-0.33%	1.8%	4.6%	0.36
Spring	4/18/2015	-1.7%	4.8%	2.9%	-3.4%	8.0%	-0.83%	3.5
Spring	4/25/2015	2.0%	-14%	-0.67%	-4.6%	3.9%	-1.1%	3.0
Spring	4/30/2015	3.8%	-23%	-3.0%	-4.4%	4.7%	-0.76%	4.9
Spring	5/9/2015	1.5%	-20%	-1.8%	-0.67%	1.7%	-0.17%	0.66
Spring	5/23/2015 11:00	3.3%	-6.6%	-3.5%	-1.8%	2.5%	-0.29%	2.9
Spring	5/30/2015 10:30	0.62%	-23%	-0.99%	0.22%	8.9%	0.49%	0.16
Spring	6/5/2015 11:00	-0.41%	-22%	1.9%	-2.6%	5.7%	0.59%	1.2
Spring	6/13/2015 8:00	0.63%	-28%	-0.59%	-0.76%	1.9%	1.7%	0.15
Spring	6/19/2015 11:00	1.3%	-22%	0.17%	-4.3%	-0.60%	-0.38%	2.4
Spring	6/28/2015 8:30	2.2%	-22%	-0.88%	-4.7%	3.0%	0.17%	3.2
Spring	7/3/2015 9:00	4.2%	-33%	-3.6%	-4.0%	3.0%	-1.1%	5.2
Spring	7/10/2015 17:30	-1.1%	-19.6%	2.9%	-2.1%	3.7%	0.60%	1.5
Spring	7/16/2015 17:00	-1.1%	-35%	2.3%	-1.1%	2.0%	0.68%	0.83
Spring	8/1/2015 10:00	-0.31%	-40%	1.2%	-1.6%	6.8%	2.5%	0.45
Spring	8/8/2015 10:00	1.7%	-43.7%	0.17%	-5.3%	-2.1%	-1.2%	3.8
Spring	9/1/2015 15:00	5.5%	-36%	-4.1%	-6.0%	3.2%	-1.8%	9.5
Spring	9/5/2015 9:30	5.5%	-45%	-4.1%	-6.0%	3.0%	-0.71%	9.6
Spring	9/12/2015 7:40	0.89%	-32%	-0.26%	-2.3%	0.88%	-0.77%	0.73
Spring	9/19/2015 7:40	5.9%	-44%	-5.3%	-4.2%	5.9%	-0.21%	9.0
Spring	9/27/2015 9:30	3.3%	-44%	-4.1%	-0.30%	0.63%	3.7%	3.2
Spring	10/2/2015 7:30	0.42%	-39%	1.4%	-4.2%	-0.85%	-1.9%	2.4
Spring	10/9/2015 7:15	0.92%	-40%	-0.30%	-2.4%	7.6%	0.99%	0.75
Spring	10/15/2015 16:40	-0.19%	-44%	0.70%	-0.92%	3.7%	1.5%	0.15
Spring	10/27/2015 8:00	2.7%	-34%	-1.3%	-5.1%	-0.38%	0.64%	4.1
Spring	10/27/2015 12:00	4.4%	-46%	-3.8%	-4.3%	4.1%	-1.0%	5.9

Table 2 cont.

Site	Date/Time	% Difference Between Measured and Theoretical						Sum χ^2
		Xe	N2	Ar	Ne	Kr	He4	
Spring	10/27/2015 16:00	1.4%	-41%	1.7%	-7.3%	8.7%	-1.6%	7.5
Spring	10/28/2015 0:00	2.8%	-46%	-4.0%	0.94%	-0.69%	1.6%	2.9
Spring	10/28/2015 4:00	3.2%	-50%	-3.8%	-0.75%	6.8%	-0.75%	2.8
Spring	10/28/2015 8:00	3.9%	-46%	-2.8%	-5.0%	0.12%	0.25%	5.5
Spring	10/28/2015 11:00	-1.2%	-30%	2.6%	-1.4%	3.3%	1.2%	1.1

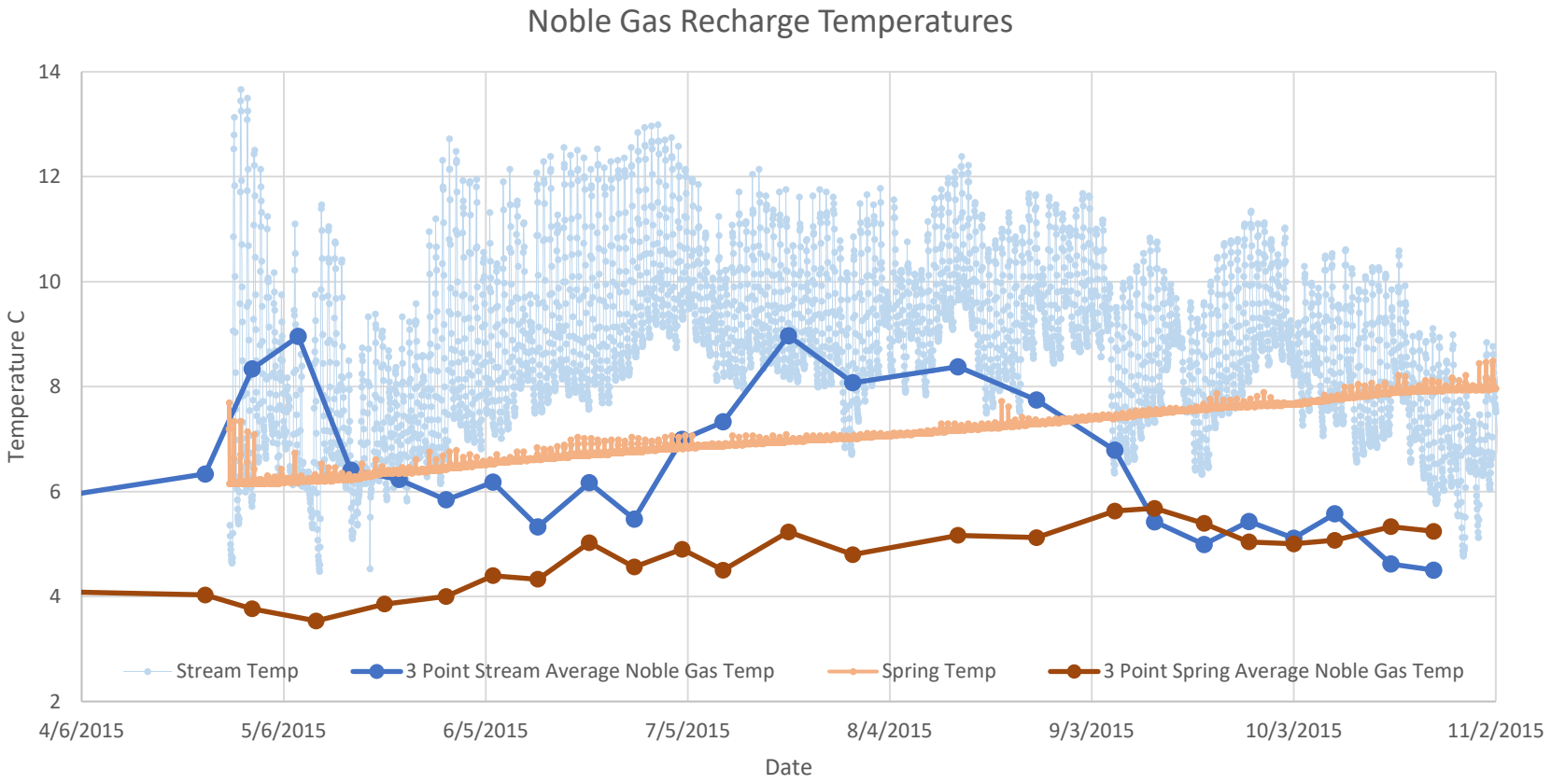

Figure 12. Spring to fall 2015 noble gas results. The thin light blue line is the measured temperature of the stream, thin orange line is the measured temperature of the spring, the dark blue line is the 3 point averaged calculated recharge temperature of the stream and the bold orange line is the 3 point averaged calculated recharge of the spring. The recharge temperature curve for the stream roughly follows the physical temperature of the stream. The upward trend of the spring's recharge temperature curve similarly tracks the upward trend of the physical temperature of the spring. Three-point averages were used to help smooth out the large variations due to samples collected at different times during the day. The complete data can be found in Appendix D.

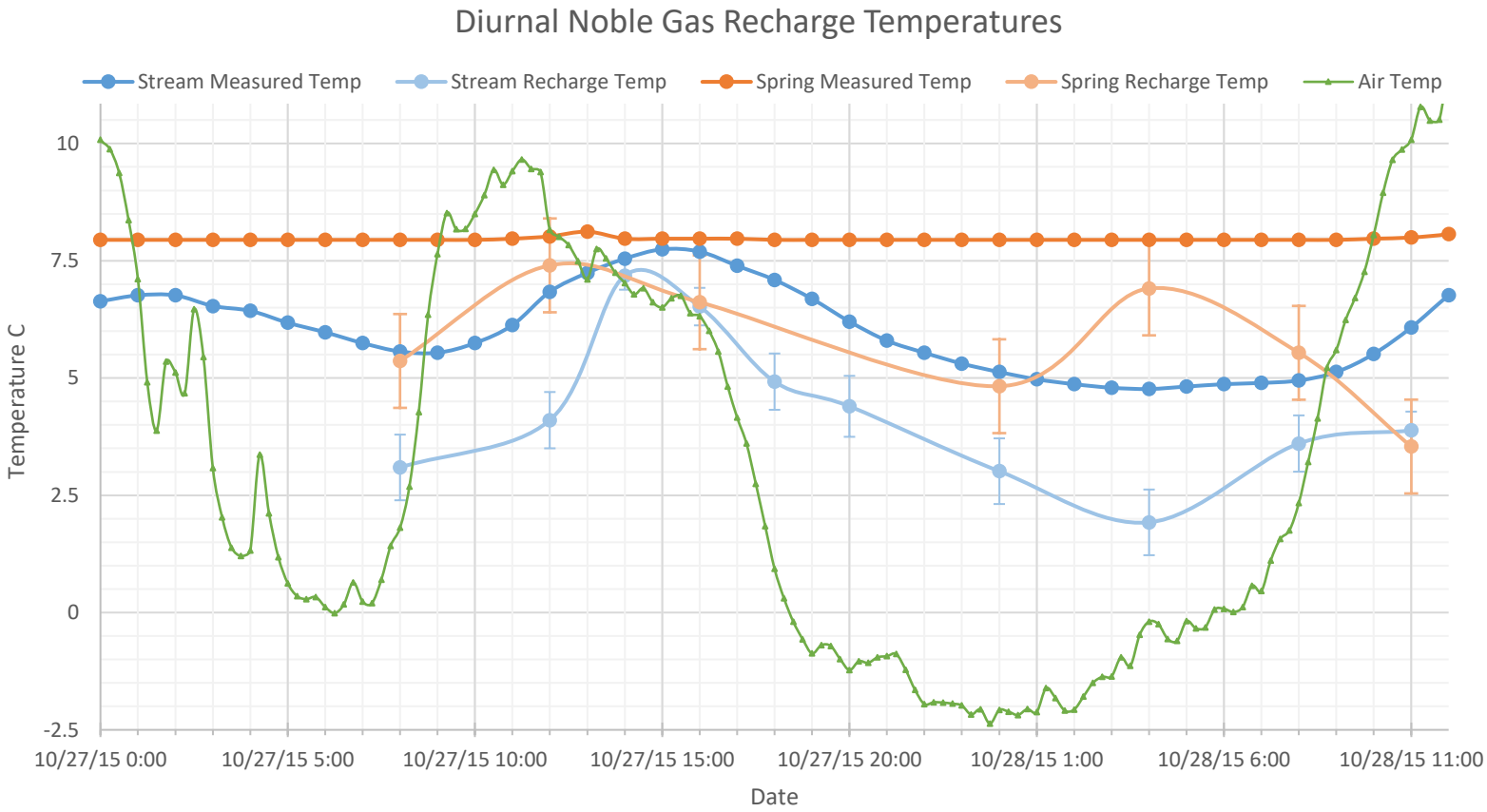

Figure 13. Diurnal noble gas results. The light blue line is the calculated recharge temperature of the stream, the blue line is the physical temperature of the stream, the light orange line is the calculated recharge temperature of the spring, the orange line is the physical temperature of the spring, and the green line is the temperature of the air. The stream recharge temperatures appear to show an intermediate value between the stream and the air temperatures. However, the spring recharge temperatures seem to mimic the air temperature with an offset of roughly 13 h, possibly due to some exposure to the atmosphere before discharging.

4 DISCUSSION AND CONCLUSION

4.1 Validity of noble gas recharge temperatures

The noble gas method stands on the assumption that the noble gas solubility is driven by the temperature of the water into which the gas dissolves. This means that the noble gas concentration is a measure of the average stream temperature and thus will remain unchanged once it becomes isolated from the atmosphere (i.e., below the water table) and thus it can be used to calculate recharge temperatures. However, as was evident from the data collected, this does not always appear to be the case. As shown during the diurnal sampling, when the air temperature and the water temperature were not the same, the apparent noble gas temperature was an intermediate value between the two temperatures and was never greater than the water temperature. When the air temperature dropped below the water temperature, the apparent recharge temperature began deviating away from the water temperature toward the air temperature. Since water has a much larger heat capacity than air, it seems reasonable to assume that the water skin temperature is the largest factor in the gas solubility under daytime conditions, but it seems that the air temperature plays a larger role when the air is colder than the water.

Another possible reason that the apparent recharge temperatures appear to deviate so much from the water temperature could be the proximity of the sampling sites to the origin of the stream. The stream in Knowltons Fork begins as several springs approximately 2 km from the injection site. It is possible that the water discharging from the Knowltons Fork

springs has not fully equilibrated with the atmosphere at the point of the injection site and thus represents an intermediate temperature between the stream temperature and the recharge temperature of the groundwater discharging from the Knowltons Fork springs.

4.2 Summary and conclusions

From this study, radon was verified as a useful tool in identifying where hyporheic flow discharges into a stream. The radon survey helped to identify two previously unknown springs. It was determined from a bromide injection test that the mean transit time of hyporheic flow through the tufa spring in upper Red Butte Creek is between 18 and 48 days. The injection test provided a reliable range of transit times and confirmed that water from the stream is discharged from the tufa. Mass balance calculations indicate that 39.8 kg of bromide were injected into the stream and 4.2 kg were discharged from the tufa spring. This suggests that roughly 10% of the stream entered the hyporheic zone and then was discharged at the tufa spring. The calculation also indicates that water discharging from the tufa spring is approximately 93% stream water with the remaining 7% being either new groundwater or water that entered the hyporheic flow path above the injection site. Thus, the spring is fed almost entirely by stream water. It is estimated that between 2,799,000 L and 7,465,000 L of water is stored within this one hyporheic zone within the canyon.

Storm events were used as “injection tests” of stable isotopes. Results from one storm in mid-July showed an approximate transit time of 16 days ± 7 days. The largest uncertainty in the measurements came from the sampling frequency. While it could not be verified that the stream achieved the same isotopic composition as the storm, it is assumed that enough

of storm water with its distinctive isotopic composition entered the hyporheic zone to allow us to see some isotopically detectable offset after dispersion. Earlier sampling efforts did not provide enough resolution to measure the difference between the stream and the spring compositions. However, with better resolution, the stable isotopes show the most potential for being able to measure transit times without performing an active injection test.

Using the stable isotope method, a transit time of 16 days was measured, about 2 days faster than the peak bromide method measured. This suggests seasonal variation in the transit time. The bromide test was conducted during base flow conditions, whereas the stable isotopes were measured during the summer months when there is more precipitation and evapotranspiration. This could affect the mean transit time and explain the difference between the transit times measured between the active and passive techniques.

Results from the noble gases were not conclusive in terms of transit time for various reasons. First, there are some potential issues with the assumption that the high heat capacity of the water controls the solubility of the noble gases. While the high heat capacity of water should control the solubility, the method assumes the air in contact with the water and the water are at the same temperature. However, since air convects, when the water is warmer than the overlying air, the air buoyantly rises away from the contact as soon as it starts to be warmed by the water and is replaced by cold air from above. Therefore, the air in contact with the water never reaches the temperature of the water, meaning the gas-solubility technique cannot be used when the ambient air is colder than the water as chemical equilibrium is never reached.

There is also the possibility that the stream water has not reached full equilibrium after discharging from the Knowltons Fork springs some 2 km upstream. This would lead to the

stream representing an intermediate temperature of stream water and the recharge temperature from the springs. The size and timing of the data population also make it difficult to calculate a transit time. While the model of noble gases traveling through the hyporheic zone indicated that we would be able to see the offset between the stream and the spring (Figure 6), the timing of the sampling was not ideal. Sampling from spring to late summer resulted in only measuring one limb of the cyclical, seasonal changes. The peak and valley were missed by the sampling. The best way to determine a transit time would be to measure either the peak or the valley of the data and measure the offset between the stream data and the spring data.

Another complication became apparent from the results of diurnal sampling. While the physical temperature of the spring remained constant, the calculated recharge temperatures from the noble gases varied considerably. One thought is that there is some reequilibration with the atmosphere inside the tufa mound before the water finally discharges. The sound of water gurgling inside the tufa mound can be heard, which would indicate exposure to the atmosphere before discharge. The results seem to show an offset of about 13 h from the air temperature and the calculated spring recharge temperatures. This could also be related to the stream not reaching equilibrium by the time the water enters the hyporheic zone. This suggests that the tufa spring may not be the best location to test the noble gas passive method.

4.3 Future studies

A follow-up study should be carried out that tests the assumption that the high heat capacity of water controls the solubility of the noble gases. A test conducted in a lab setting

where the water is maintained at a certain temperature and the air temperature is changed to see if there are any effects on the solubility of the noble gases, especially when the air is much colder than the water temperature might provide the information required.

To further determine if the noble gases can be used to date young groundwater/hyporheic flows, more data from a hyporheic spring and the stream that captures either the peak or valley of the seasonal changes could help verify the noble gas technique. Ideally, collecting samples for an entire year would provide such data as well as measuring both the peak and the valley to see if they yield similar estimated transit times.

APPENDIX A

RADON DATA

Table 3. Complete radon sampling data

Location	Sample Date	Meters from Start	Radon (PiC/L)	St. Dev
RB-0	10/21/13	0	46	19
Up 1	10/21/13	110	33	15
RB-163	10/21/13	165	8.9	9.2
Inflow up*	10/21/13	200	770	82
RB-279	10/21/13	256	150	34
RB-376	10/21/13	361	94	14
RB-3232	10/22/13	3232	6.7	0.01
Parley's Inflow*	10/22/13	3700	5.0	4.1
RB-4133	10/22/13	4133	6.7	0.01
Gage Station	10/22/13	4900	5.0	2.1
RB-580	10/23/13	569	20	10
RB-746	10/23/13	727	5.4	5.3
RB-868	10/23/13	855	41	17
RB-988	10/23/13	965	22	8.5
RB-1090	10/23/13	1087	29	11
RB-1343	10/23/13	1306	21	12
RB-1592	10/23/13	1570	6.7	5.5
RB-1715	10/23/13	1704	64	17
RB-1902	10/23/13	1905	33	10
RB-2266	10/23/13	2266	17	5.5
RB-2725	10/23/13	2725	6.2	8.0
RB-3564	10/23/13	3564	3.8	4.1
RB 988	11/9/13	969	17	11
11	11/9/13	1024	9.2	5.5
RB 1090	11/9/13	1087	32	18
10	11/9/13	1151	17	9.4
RB 1902	11/9/13	1905	28	7.3
1	11/9/13	1866	30	11
2	11/9/13	1828	49	19
3	11/9/13	1792	31	13
4	11/9/13	1755	68	15

Table 3 cont.

Location	Sample Date	Meters from Start	Radon (PiC/L)	St. Dev
RB 1715	11/9/13	1704	38	7.7
5	11/9/13	1633	11	2.1
6	11/9/13	1613	13	6.0
RB 1592	11/9/13	1570	8.0	5.3
7	11/9/13	1509	16	10
8	11/9/13	1452	1.6	2.1
13	11/13/13	641	45	26
RB 580	11/13/13	569	53	17
14	11/13/13	527	68	22
16 Spr	11/13/13	786	730	30
16	11/13/13	783	51	9.4
15	11/13/13	427	88	18
RB 376	11/13/13	361	120	38
17	11/13/13	326	130	14
Inflow*	11/13/13	200	940	88
RB 163	11/13/13	165	48	8.8
UP 1	11/13/13	110	48	11
RB 0	11/13/13	0	73	21
Main 0	11/13/13	0	52	9.8
RB 965	11/13/13	969	76	16
RB 1902	11/13/13	1905	84	10
RB 279	11/13/13	256	160	28
2010 Inj	11/13/13	453	61	19
RB 746	11/13/13	727	4.9	3.5
RB 863	11/13/13	855	30	15
12	11/13/13	890	27	11
RB 279	2/21/14	279	160	29
RB 580	2/21/14	580	21	14
2010 Inj	2/21/14	453	48	13
Just Below Spring 16	2/21/14	788	41	14
Just Above Spring 16	2/21/14	780	41	16

Table 3 cont.

Location	Sample Date	Meters from Start	Radon (PiC/L)	St. Dev
RB 988	2/21/14	988	49	14
RB 0	3/7/14	0	23	7.3
RB 1	3/7/14	20	13	3.4
RB 2	3/7/14	40	12	4.1
RB 3	3/7/14	60	14	13
RB 4	3/7/14	80	11	4.1
RB 5	3/7/14	100	5.1	6.0
RB 6	3/7/14	120	2.6	2.5
RB 7	3/7/14	140	0.0	0.0
RB 8	3/7/14	160	1.3	2.1
RB 9	3/7/14	180	12	2.1
RB 10	3/7/14	200	17	5.5
Spring Up	3/7/14	200	550	62
Spring Inflow	3/7/14	200	390	26
RB 279	3/7/14	279	140	24
Spring 16	3/7/14	760	690	39

APPENDIX B

BROMIDE INJECTION TEST DATA

For the bromide injection test, a bromide solution had to be mixed. An injection concentration of 260,000 mg/L was achieved by dissolving 110 lbs of NaBr into 41 gallons (~155 L) of water. The solution was mixed in a large water tank situated at the top of a small waterfall. A pump, connected to batteries, was attached to the tank that discharged the solution into the waterfall to facilitate rapid mixing with the stream water. The pump discharged at approximately 100 mL/min.

Around 8:50 am, a very small leak was found at the connection of the tank to the pump. The leak was small (about 1 mL every 15 min) and was assumed to have occurred throughout the night. Not much injectant was lost, and a bucket was placed under the leak to prevent any further leakage from entering the ground. Another issue occurred with the pump itself. It was found that, due to a programming error, the pump would turn itself off after so many revolutions (approximately every 30-40 min). When this was first noticed, it is estimated that the pump had been off for approximately 20 min. The pump had to be restarted several times throughout the day until the programming error could be corrected. When the pump was checked early the next morning after running all night, it was found that the pump was only pumping approximately 50 mL/min. This most likely occurred gradually throughout the night as the pump slowly drained the energy from the batteries. The pumping rate was increased back to 100 mL/min and, after 26 h of pumping, the rate was increased to 130 mL/min to empty out the remaining bromide solution.

Table 4. Calculations for determining amount of bromide to use

Red Butte Canyon		**Br as NaBr**
Tracer:		Each injection Br as NaBr
Distance		1.9
Start:		10/8/2014 10:30
End:		10/9/2014 15:30
Duration of tracer (hours):		26.0
Gram formula weight of tracer:		79.909
Gram formula weight of salt:		102.899
Tracer percent:		78%
Cost per pound:	$	2.31
Pounds per unit cost:		55.1
Maximum stream discharge (cfs):		**1.0**
Maximum stream discharge (L/s):		**28.3**
Minimum tracer concentration goal (mg/L):		**15.00**
Alternate concentration (mg/L):		**3.35**
Conc of injectate (mg/L):		**256,439**
Mass flux (mg/s):		424.76
Mass flux of pump (mg/s):		424.76
Pump rate (mL/min):		99.4
Total volume injected (gallons):		41.0
Total volume injected (liters):		155.0
Mass of tracer (kg):		39.8
Mass of total salt (lb.):		**112.9**
Mass of total salt (kg):		51.2
Bags (55 lb.):		2.0
Mixture (lb./30 gal garbage can):		82.7
Garbage Cans:		1.4
Tanks:		0.20
Cost	$	260.77

Table 5. Ion chromatograph results from the tufa spring during the injection test

Date/Time	Bromide (mg/L)	Fluoride (mg/L)	Chloride (mg/L)	Nitrate (mg/L)	Sulfate (mg/L)
11/11/2014 7:53	0.11	0.12	7.59	3.83	79.9
11/11/2014 10:48	0.13	0.13	7.33	0.19	79.0
11/11/2014 13:53	0.30	0.11	7.52	0.06	79.7
11/12/2014 13:53	0.00	0.11	7.57	0.08	80.1
11/13/2014 14:28	0.00	0.12	7.36	0.19	80.2
11/14/2014 11:10	0.00	0.12	7.46		80.9
11/14/2014 13:53	0.00	0.11	7.55	0.09	80.3
11/15/2014 1:53	0.00	0.12	7.44		81.0
11/15/2014 7:53	0.00	0.12	7.45	0.21	80.9
11/15/2014 13:53	0.00	0.12	7.45		80.4
11/15/2014 16:57	0.00	0.12	7.49		81.4
11/15/2014 19:53	0.00	0.12	7.44		80.9
11/16/2014 1:53	0.00	0.12	7.46	0.09	80.9
11/16/2014 7:53	0.00	0.12	7.44	0.18	80.8
11/16/2014 13:53	0.00	0.12	7.46	0.21	81.0
11/16/2014 19:53	0.00	0.12	7.47	0.17	81.0
11/17/2014 1:53	0.00	0.12	7.47	0.08	81.4
11/17/2014 20:01	0.00	0.12	7.49	0.23	80.9
11/18/2014 2:01	0.00	0.12	7.47	0.09	81.1
11/18/2014 8:01	0.00	0.12	7.40	0.08	80.3
11/18/2014 14:01	0.00	0.12	7.45	0.08	80.9
11/18/2014 21:00	0.00	0.11	7.55		81.5
11/19/2014 9:00	0.14	0.13	7.41	0.18	80.1
11/19/2014 21:00	0.15	0.13	7.42	0.19	80.2
11/20/2014 9:00	0.17	0.13	7.43	0.18	80.0
11/20/2014 21:00	0.20	0.12	7.37	0.17	79.9
11/21/2014 9:00	0.22	0.13	7.34	0.18	79.5
11/29/2014 11:00	0.41	0.13	7.34	0.08	78.6
11/29/2014 11:05	0.66	0.12	7.44	0.19	80.1
11/29/2014 23:00	0.41	0.13	7.32	0.07	78.5
11/30/2014 11:00	0.40	0.13	7.32	0.18	78.4
11/30/2014 23:00	0.40	0.13	7.32	0.13	78.4

Table 5 cont.

Date/Time	Bromide (mg/L)	Fluoride (mg/L)	Chloride (mg/L)	Nitrate (mg/L)	Sulfate (mg/L)
12/1/2014 11:00	0.41	0.13	7.32	0.11	78.4
12/1/2014 15:39	0.59	0.12	7.40	0.14	79.4
12/1/2014 21:00	0.59	0.12	7.40	0.10	79.5
12/2/2014 9:00	0.58	0.12	7.42	0.14	79.5
12/2/2014 21:00	0.56	0.12	7.42	0.13	79.6
12/3/2014 9:00	0.55	0.12	7.42	0.13	79.5
12/3/2014 21:00	0.54	0.12	7.42	0.12	79.6
12/4/2014 9:00	0.54	0.12	7.42	0.13	79.5
12/4/2014 21:00	0.54	0.12	7.43	0.09	79.5
12/5/2014 9:00	0.53	0.13	7.42	0.16	79.4
12/5/2014 12:47	0.44	0.11	7.51	0.13	79.4
12/5/2014 14:00	0.42	0.11	7.52	0.11	79.5
12/6/2014 14:00	0.42	0.11	7.53	0.11	79.4
12/7/2014 14:00	0.40	0.11	7.49	0.11	79.1
12/8/2014 14:00	0.40	0.11	7.47	0.21	78.8
12/9/2014 14:00	0.38	0.11	7.44	0.11	78.6
12/10/2014 14:00	0.38	0.11	7.44	0.11	78.4
12/11/2014 14:00	0.37	0.11	7.48	0.11	78.6
12/12/2014 14:00	0.36	0.13	7.38	0.19	78.2
12/13/2014 14:00	0.35	0.12	7.38	0.17	78.2
12/14/2014 14:00	0.34	0.13	7.41	0.15	78.1
12/15/2014 14:00	0.33	0.12	7.40	0.14	78.1
12/16/2014 14:00	0.33	0.12	7.43	0.09	78.1
12/17/2014 14:00	0.32	0.12	7.39	0.18	78.0
12/18/2014 11:30	0.30	0.03	7.57	0.22	71.7
12/18/2014 14:00	0.28	0.04	7.55	0.18	72.0
12/19/2014 14:00	0.27	0.04	7.63	0.19	73.6
12/20/2014 14:00	0.27	0.05	7.75	0.23	75.7
12/21/2014 14:00	0.27	0.05	7.77	0.13	76.6
12/22/2014 14:00	0.26	0.05	8.15	0.15	78.5
12/23/2014 14:00	0.24	0.06	7.54	0.18	74.9
12/24/2014 14:00	0.25	0.06	7.55	0.15	76.6

Table 5 cont.

Date/Time	Bromide (mg/L)	Fluoride (mg/L)	Chloride (mg/L)	Nitrate (mg/L)	Sulfate (mg/L)
12/25/2014 14:00	0.23	0.06	7.83	0.16	77.3
12/26/2014 14:00	0.24	0.07	7.53	0.20	77.3
12/27/2014 14:00	0.24	0.07	7.76	0.22	77.6
12/28/2014 14:00	0.24	0.08	7.79	0.18	77.7
12/29/2014 14:00	0.24	0.09	7.68	0.23	78.6
12/30/2014 14:00	0.22	0.11	7.59	0.14	78.3
12/31/2014 14:00	0.22	0.12	7.58	0.15	78.7
1/1/2015 14:00	0.23	0.12	7.82	0.13	79.0
1/2/2015 14:00	0.21	0.12	9.22	0.13	78.2
1/3/2015 14:00	0.23	0.12	7.69	0.17	78.6
1/4/2015 14:00	0.26	0.13	7.42	0.25	78.1
1/5/2015 14:00	0.27	0.12	7.36	0.30	78.0
1/6/2015 14:00	0.27	0.12	7.32	0.31	77.3
1/7/2015 14:00	0.26	0.12	7.30	0.31	76.9
1/8/2015 14:00	0.27	0.12	7.58	0.35	77.1
1/9/2015 14:00	0.25	0.12	7.35	0.32	77.2
1/19/2015 10:54	0.22	0.12	7.36	0.32	77.0
1/26/2015 14:44	0.15	0.12	7.69	0.33	76.8
3/13/2015 14:21	0.14	0.13	7.69	0.25	78.3

Table 6. Ion chromatograph results from the lower spring during the injection test

Date/Time	Bromide (mg/L)	Fluoride (mg/L)	Chloride (mg/L)	Nitrate (mg/L)	Sulfate (mg/L)
11/11/2014 7:53	0.00	0.08	8.84		71.23
11/11/2014 10:40	0.00	0.11	8.08	0.07	62.85
11/11/2014 13:53	0.00	0.10	8.47	0.08	67.47
11/11/2014 19:53	0.00	0.11	8.32	0.09	65.96
11/11/2014 21:00	0.00	0.11	8.25		65.46
11/12/2014 1:53	0.00	0.11	8.30	0.08	66.18
11/12/2014 7:53	0.00	0.10	8.23	0.09	65.17
11/12/2014 13:53	0.00	0.10	8.32		66.46
11/12/2014 19:53	0.00	0.10	8.09	0.09	63.59
11/13/2014 1:53	0.00	0.10	8.07	0.15	63.34
11/13/2014 13:53	0.00	0.09	8.03	0.26	63.08
11/13/2014 13:53	0.00	0.10	8.23	0.09	63.58
11/13/2014 14:13	0.16	0.10	8.20	0.10	64.81
11/14/2014 7:53	0.00	0.10	8.27	0.06	63.72
11/14/2014 13:53	0.00	0.10	8.14	0.08	64.16
11/14/2014 19:53	0.00	0.10	8.44		67.36
11/15/2014 13:53	0.00	0.10	8.33	0.09	65.13
11/15/2014 7:53	0.00	0.10	8.07		63.69
11/16/2014 16:53	0.00	0.10	8.31	0.08	63.72
11/17/2014 15:15	0.00	0.10	8.28	0.65	64.29
11/18/2014 13:50	0.00	0.11	8.09	0.29	63.62
11/18/2014 16:00	0.00	0.10	8.31	0.08	64.03
11/18/2014 21:00	0.16	0.10	8.17	0.11	64.00
11/19/2014 14:17	0.00	0.10	8.26	0.08	63.97
11/19/2014 21:00	0.10	0.11	8.09	0.29	63.62
11/20/2014 9:00	0.10	0.11	8.07	0.27	63.56
11/20/2014 21:00	0.10	0.11	8.06	0.27	63.54
11/21/2014 9:00	0.11	0.11	8.07	0.26	63.78
11/21/2014 21:00	0.11	0.11	8.03	0.27	63.21
11/22/2014 9:00	0.11	0.12	8.05	0.27	63.24
11/22/2014 21:00	0.11	0.11	8.04	0.27	63.26
11/23/2014 9:00	0.11	0.11	8.04	0.27	63.38
11/23/2014 21:00	0.12	0.11	8.05	0.27	63.37

Table 6 cont.

Date/Time	Bromide (mg/L)	Fluoride (mg/L)	Chloride (mg/L)	Nitrate (mg/L)	Sulfate (mg/L)
11/24/2014 9:00	0.12	0.12	8.05	0.26	63.42
11/24/2014 21:00	0.12	0.11	8.05	0.27	63.36
11/25/2014 9:00	0.12	0.11	8.06	0.26	63.42
11/25/2014 21:00	0.12	0.11	8.01	0.26	63.25
11/26/2014 9:00	0.12	0.11	8.02	0.27	63.31
11/26/2014 21:00	0.12	0.11	8.03	0.27	63.39
11/27/2014 9:00	0.12	0.11	8.04	0.26	63.43
11/27/2014 21:00	0.12	0.12	8.05	0.27	63.49
11/28/2014 9:00	0.12	0.12	8.04	0.26	63.51
11/28/2014 21:00	0.13	0.12	8.06	0.29	63.50
11/29/2014 9:00	0.13	0.11	8.03	0.26	63.66
11/29/2014 11:29	0.24	0.10	8.30	0.07	64.29
11/29/2014 21:00	0.13	0.12	8.03	0.27	63.55
11/30/2014 9:00	0.13	0.11	8.04	0.26	63.55
11/30/2014 21:00	0.21	0.11	8.04	0.26	63.52
12/1/2014 9:00	0.14	0.11	8.02	0.28	63.58
12/1/2014 15:53	0.22	0.10	8.12	0.26	64.45
12/1/2014 21:00	0.22	0.11	8.12	0.25	64.48
12/2/2014 9:00	0.23	0.10	8.11	0.26	64.49
12/2/2014 9:00	0.15	0.09	8.68	0.10	63.57
12/2/2014 21:00	0.23	0.10	8.11	0.26	64.51
12/3/2014 9:00	0.23	0.11	8.13	0.26	64.62
12/3/2014 21:00	0.23	0.10	8.15	0.26	64.56
12/4/2014 9:00	0.23	0.10	8.11	0.26	64.50
12/4/2014 21:00	0.23	0.11	8.11	0.26	64.56
12/5/2014 9:00	0.23	0.10	8.12	0.26	64.57
12/5/2014 12:53	0.20	0.09	8.22	0.56	64.56
12/5/2014 14:00	0.19	0.10	8.20	0.38	64.61
12/6/2014 14:00	0.19	0.10	8.22	0.72	64.58
12/7/2014 14:00	0.19	0.10	8.22	1.04	64.61
12/8/2014 14:00	0.19	0.10	8.23	1.04	64.85
12/9/2014 14:00	0.20	0.10	8.25	0.81	64.84

Table 6 cont.

Date/Time	Bromide (mg/L)	Fluoride (mg/L)	Chloride (mg/L)	Nitrate (mg/L)	Sulfate (mg/L)
12/10/2014 13:00	0.23	0.12	8.22	0.24	65.03
12/10/2014 14:00	0.20	0.10	8.22	0.91	64.75
12/11/2014 14:00	0.17	0.10	8.24	1.15	64.36
12/12/2014 14:00	0.17	0.10	8.18	0.86	64.51
12/13/2014 14:00	0.17	0.11	8.14	0.50	64.35
12/14/2014 14:00	0.18	0.11	8.15	0.94	64.38
12/15/2014 14:00	0.17	0.10	8.22	0.39	64.24
12/16/2014 14:00	0.17	0.10	8.15	0.87	64.39
12/17/2014 14:00	0.18	0.11	8.14	0.37	64.38
1/19/2015 11:15	0.24	0.11	8.25	0.32	65.72
1/24/2015 21:00	0.12	0.09	8.76	0.09	64.22
1/26/2015 16:00	0.19	0.11	8.39	0.33	65.39
1/27/2015 14:00	0.20	0.12	8.62	0.26	65.73
1/28/2015 14:00	0.12	0.10	8.49	0.06	0.10
1/29/2015 14:00	0.20	0.10	8.49	0.08	65.58
1/30/2015 14:00	0.20	0.10	8.83	0.07	65.46
1/31/2015 14:00	0.20	0.10	8.64	0.07	65.54
2/1/2015 14:00	0.21	0.10	8.41		65.46
2/2/2015 14:00	0.27	0.11	8.25	0.20	64.18
2/3/2015 14:00	0.20	0.11	8.14	0.54	64.37
2/4/2015 14:00	0.19	0.10	8.70	0.08	65.52
2/5/2015 14:00	0.20	0.09	8.55	0.08	65.31
2/6/2015 14:00	0.16	0.09	8.44	0.07	
2/7/2015 14:00	0.21	0.11	8.21	0.13	64.65
2/7/2015 14:00	0.18	0.09	8.43	0.07	65.37
2/8/2015 14:00	0.16	0.10	8.73	0.08	0.10
2/9/2015 14:00	0.16	0.10	8.51	0.08	
2/10/2015 14:00	0.20	0.10	8.39	0.06	65.55
2/11/2015 14:00	0.19	0.10	8.58	0.10	65.82
2/12/2015 14:00	0.19	0.10	9.67	0.07	65.31
2/13/2015 14:00	0.20	0.09	8.65	0.08	65.82
2/14/2015 14:00	0.20	0.11	8.11	0.19	64.35

Table 6 cont.

Date/Time	Bromide (mg/L)	Fluoride (mg/L)	Chloride (mg/L)	Nitrate (mg/L)	Sulfate (mg/L)
2/15/2015 14:00	0.19	0.10	8.58	0.09	65.39
2/16/2015 9:25	0.15	0.10	8.17	0.07	64.37
3/13/2015 14:05	0.18	0.11	8.62	0.24	64.31

APPENDIX C

STABLE ISOTOPE DATA

Table 7. Stable isotope results from the stream

Date	δ18O	δ2H	δ18O_sd	δ2H_sd
2/1/14	-16.97	-125.48	0.02	0.10
3/7/14	-16.78	-125.02	0.02	0.07
3/21/14	-16.76	-125.18	0.16	0.33
4/12/14	-16.58	-123.56	0.02	0.32
4/29/14	-16.73	-125.06	0.03	0.09
6/4/14	-16.73	-124.74	0.04	0.11
6/18/14	-16.87	-125.00	0.04	0.19
7/17/14	-17.02	-126.18	0.05	0.24
7/31/14	-17.00	-126.15	0.02	0.04
8/21/14	-16.88	-124.42	0.02	0.20
9/3/14	-16.88	-125.17	0.06	0.17
9/17/14	-16.81	-124.70	0.07	0.17
10/10/14	-16.93	-124.89	0.03	0.06
10/22/14	-17.07	-125.93	0.04	0.13
11/14/14	-16.95	-125.88	0.03	0.06
11/19/14	-16.82	-124.90	0.03	0.02
12/10/14	-16.84	-125.37	0.04	0.03
4/30/15	-14.70	-118.2	0.02	0.12
5/9/15	-15.70	-121.9	0.02	0.05
5/16/15	-16.02	-122.2	0.02	0.20
5/23/15	-13.17	-113.5	0.03	0.08
5/30/15	-16.73	-124.1	0.03	0.07
6/5/15	-16.72	-124.5	0.03	0.05
6/13/15	-16.77	-124.7	0.02	0.06
6/19/15	-16.79	-124.7	0.01	0.04
6/28/15	-16.77	-124.9	0.03	0.08
7/3/15	-16.78	-124.7	0.02	0.09
7/10/15	-16.88	-124.9	0.03	0.14
7/16/15	-14.74	-119.0	0.03	0.08
8/1/15	-15.72	-121.6	0.03	0.02
8/8/15	-16.13	-122.9	0.01	0.06
9/1/15	-16.74	-125.2	0.06	0.36
9/5/15	-16.91	-125.6	0.06	0.23

Table 8. Stable isotope results from the tufa spring

Date	δ18O	δ2H	δ18O_sd	δ2H_sd
3/7/14	-16.85	-125.40	0.03	0.14
3/21/14	-16.85	-125.42	0.02	0.08
4/12/14	-16.84	-124.95	0.01	0.21
4/29/14	-16.73	-124.49	0.03	0.13
6/4/14	-16.36	-123.68	0.07	0.22
6/18/14	-16.73	-124.29	0.03	0.08
7/17/14	-16.84	-125.20	0.02	0.13
7/31/14	-16.87	-125.60	0.01	0.08
8/21/14	-16.72	-124.19	0.02	0.06
9/3/14	-16.78	-124.73	0.03	0.17
9/17/14	-16.75	-124.59	0.02	0.07
10/10/14	-16.90	-124.45	0.09	0.33
10/22/14	-16.97	-125.47	0.03	0.12
11/14/14	-16.83	-125.24	0.03	0.18
11/19/14	-16.57	-124.19	0.02	0.08
12/10/14	-16.88	-125.24	0.01	0.07
4/30/15	-15.45	-121.0	0.02	0.07
5/9/15	-16.18	-123.2	0.02	0.08
5/16/15	-15.87	-122.2	0.01	0.05
5/23/15	-15.67	-122.0	0.02	0.12
5/30/15	-15.85	-122.1	0.02	0.09
6/5/15	-16.63	-124.2	0.03	0.02
6/13/15	-16.66	-124.3	0.03	0.05
6/19/15	-16.64	-124.2	0.04	0.15
6/28/15	-16.63	-123.8	0.03	0.16
7/3/15	-16.63	-123.9	0.01	0.07
7/10/15	-16.71	-124.3	0.01	0.06
7/16/15	-15.60	-120.9	0.01	0.14
8/1/15	-15.24	-119.8	0.02	0.07
8/8/15	-16.06	-122.3	0.00	0.08
9/1/15	-16.38	-123.4	0.15	0.42
9/5/15	-16.67	-124.3	0.02	0.07

Table 9. Precipitation data from the University of Utah during 2015

Start Date	End Date	Date (average)	Avg 18O	Avg 2H	Volume	Notes
3/3/2015	3/11/2015	3/7/2015	-21.38	-163.38	54.72	Rain
3/11/2015	3/27/2015	3/20/2015	-12.7	-96.79	42.1	Rain
3/27/2015	4/9/2015	4/8/2015	-19.51	-142.86	97.46	Rain/snow on 4/8/15
4/9/2015	4/17/2015	4/15/2015	-13.52	-93.76	211.77	Rain/snow associated w/ big cold front on 4/14-15/15
4/17/2015	4/24/2015	4/20/2015	-1.9	-11.6	3.79	First ~20 min of rain from system arriving today
4/24/2015	4/27/2015	4/25/2015	-15.51	-113.48	245.51	Weekend rainstorms, mostly on 4/24 and 25
4/27/2015	5/4/2015	5/1/2015	-0.06	-12.2	29.58	Weekend thundershowers
5/4/2015	5/6/2015	5/5/2015	-5.59	-37.25	30.74	Overnight rainstorm
5/6/2015	5/8/2015	5/7/2015	-9.83	-65.99	198.71	Thundershowers
5/8/2015	5/18/2015	5/15/2015	-15.65	-116.42	500.23	Rain showers; bottle full to capacity, may have had spill-over
5/18/2015	5/19/2015	5/18/2015	-13.3	-95.19	84.25	Tshowers of evening of 18th
5/19/2015	5/26/2015	5/22/2015	-9.68	-72.78	48.59	Rain showers
5/26/2015	5/26/2015	5/26/2015	-10.5	-82.72	16.49	Light pm rain showers
5/26/2015	6/9/2015	6/2/2015	-11.93	-91.82	121.09	rain/thunder showers collected after long time, might be chance of evaporation
6/9/2025	7/8/2015	6/24/2015	-6.46	-52.78	95.41	Rain
7/8/2015	7/10/2015	7/9/2015	-9.69	66.77	111.82	Rain/thunder showers
7/10/2015	7/21/2015	7/16/2015	-5.98	-54.15	7.55	Rain
7/21/2015	8/4/2015	7/28/2015	-9.33	-70.75	82.18	Rain
8/4/2015	8/10/2015	8/7/2015	-9.21	-60.44	109.92	Rain

APPENDIX D

NOBLE GAS DATA

Table 10. Noble gas data for site RB-0

Date and Time	Water Temp (C)	Recharge Temp (C)	Xe Meas. (ccSTP/g)	Xe Theor. (ccSTP/g)	Ar Meas. (ccSTP/g)	Ar Theor. (ccSTP/g)	Ne Meas. (ccSTP/g)	Ne Theor. (ccSTP/g)	Kr Meas. (ccSTP/g)	Kr Theor. (ccSTP/g)	He4 Meas. (ccSTP/g)	He4 Theor. (ccSTP/g)
11/5/14 12:00	7.60	8.89	1.08E-08	1.08E-08	3.18E-04	3.13E-04	1.56E-07	1.61E-07	7.82E-08	7.42E-08	3.65E-08	3.68E-08
4/18/15 12:00	7.50	2.73	1.36E-08	1.36E-08	3.70E-04	3.65E-04	1.67E-07	1.72E-07	9.78E-08	8.97E-08	3.85E-08	3.81E-08
4/25/15 12:00	6.90	3.87	1.31E-08	1.30E-08	3.56E-04	3.54E-04	1.64E-07	1.70E-07	8.59E-08	8.65E-08	3.82E-08	3.78E-08
4/30/15 12:00	8.50	12.40	9.64E-09	9.56E-09	2.89E-04	2.88E-04	1.51E-07	1.56E-07	7.17E-08	6.71E-08	3.56E-08	3.63E-08
5/9/15 12:00	6.50	8.75	1.11E-08	1.09E-08	3.15E-04	3.14E-04	1.46E-07	1.61E-07	7.87E-08	7.45E-08	3.35E-08	3.69E-08
5/15/15 12:00	7.80	5.71	1.19E-08	1.21E-08	3.57E-04	3.38E-04	1.61E-07	1.66E-07	9.18E-08	8.16E-08	3.73E-08	3.74E-08
5/23/15 11:00	7.60	4.77	1.26E-08	1.26E-08	3.53E-04	3.46E-04	1.61E-07	1.68E-07	8.49E-08	8.41E-08	3.72E-08	3.76E-08
5/30/15 10:30	8.70	8.21	1.10E-08	1.13E-08	3.44E-04	3.27E-04	1.63E-07	1.68E-07	7.93E-08	7.76E-08	3.77E-08	3.83E-08
6/5/15 11:00	8.37	4.55	1.28E-08	1.27E-08	3.52E-04	3.48E-04	1.62E-07	1.68E-07	8.50E-08	8.46E-08	3.76E-08	3.77E-08
6/13/15 8:00	9.80	5.77	1.24E-08	1.21E-08	3.31E-04	3.38E-04	1.63E-07	1.66E-07	9.02E-08	8.15E-08	3.75E-08	3.74E-08
6/19/15 11:00	9.05	5.66	1.22E-08	1.22E-08	3.39E-04	3.38E-04	1.64E-07	1.66E-07	8.67E-08	8.18E-08	3.72E-08	3.74E-08
6/28/15 8:30	8.67	7.07	1.19E-08	1.16E-08	3.20E-04	3.27E-04	1.56E-07	1.64E-07	8.44E-08	7.83E-08	3.68E-08	3.72E-08
7/3/15 9:00	8.99	3.70	1.42E-08	1.31E-08	3.29E-04	3.56E-04	1.64E-07	1.70E-07	8.71E-08	8.69E-08	3.80E-08	3.79E-08
7/10/15 17:30	9.72	10.21	1.02E-08	1.04E-08	3.22E-04	3.07E-04	1.57E-07	1.61E-07	8.14E-08	7.21E-08	3.66E-08	3.71E-08
7/16/15 17:00	11.1	8.08	1.10E-08	1.11E-08	3.29E-04	3.19E-04	1.57E-07	1.62E-07	7.49E-08	7.60E-08	3.68E-08	3.70E-08
8/1/15 10:00	9.80	8.63	1.09E-08	1.09E-08	3.18E-04	3.15E-04	1.57E-07	1.61E-07	7.82E-08	7.48E-08	3.64E-08	3.69E-08
8/8/15 10:00	9.50	7.52	1.14E-08	1.14E-08	3.29E-04	3.23E-04	1.58E-07	1.63E-07	7.95E-08	7.73E-08	3.67E-08	3.71E-08
9/1/15 15:00	11.43	8.99	1.10E-08	1.08E-08	3.07E-04	3.12E-04	1.55E-07	1.61E-07	7.36E-08	7.40E-08	3.66E-08	3.68E-08

Table 10 cont.

Date and Time	Water Temp (C)	Recharge Temp (C)	Xe Meas. (ccSTP/g)	Xe Theor. (ccSTP/g)	Ar Meas. (ccSTP/g)	Ar Theor. (ccSTP/g)	Ne Meas. (ccSTP/g)	Ne Theor. (ccSTP/g)	Kr Meas. (ccSTP/g)	Kr Theor. (ccSTP/g)	He4 Meas. (ccSTP/g)	He4 Theor. (ccSTP/g)
9/5/15 9:30	8.85	6.72	1.18E-08	1.17E-08	3.34E-04	3.30E-04	1.56E-07	1.65E-07	8.46E-08	7.91E-08	3.72E-08	3.72E-08
9/12/15 7:40	7.04	4.65	1.30E-08	1.27E-08	3.40E-04	3.47E-04	1.63E-07	1.68E-07	8.45E-08	8.44E-08	3.74E-08	3.77E-08
9/19/15 7:40	6.07	4.91	1.26E-08	1.25E-08	3.47E-04	3.45E-04	1.62E-07	1.68E-07	8.80E-08	8.37E-08	3.73E-08	3.76E-08
9/27/15 9:30	8.24	5.42	1.28E-08	1.23E-08	3.29E-04	3.41E-04	1.60E-07	1.67E-07	8.27E-08	8.24E-08	3.69E-08	3.75E-08
10/2/15 7:30	3.01	5.96	1.23E-08	1.20E-08	3.30E-04	3.36E-04	1.61E-07	1.66E-07	8.36E-08	8.10E-08	3.62E-08	3.74E-08
10/9/15 7:15	7.05	3.95	1.32E-08	1.30E-08	3.53E-04	3.54E-04	1.62E-07	1.70E-07	8.51E-08	8.62E-08	3.75E-08	3.78E-08
10/15/15 16:40	9.88	6.81	1.19E-08	1.17E-08	3.24E-04	3.29E-04	1.59E-07	1.64E-07	7.89E-08	7.89E-08	3.63E-08	3.72E-08
10/27/15 8:00	5.33	3.09	1.40E-08	1.34E-08	3.47E-04	3.62E-04	1.67E-07	1.71E-07	9.00E-08	8.86E-08	3.73E-08	3.80E-08
10/27/15 12:00	6.80	4.10	1.31E-08	1.29E-08	3.54E-04	3.52E-04	1.61E-07	1.69E-07	8.76E-08	8.58E-08	3.71E-08	3.78E-08
10/27/15 14:00	7.38	7.18	1.21E-08	1.15E-08	3.16E-04	3.26E-04	8.23E-08	7.80E-08	8.23E-08	7.80E-08	3.68E-08	3.72E-08
10/27/15 16:00	7.55	6.52	1.23E-08	1.18E-08	3.26E-04	3.31E-04	1.51E-07	1.65E-07	8.00E-08	7.96E-08	3.67E-08	3.73E-08
10/27/15 18:00	6.82	4.92	1.25E-08	1.25E-08	3.53E-04	3.45E-04	1.61E-07	1.68E-07	8.53E-08	8.36E-08	3.68E-08	3.76E-08
10/27/15 20:00	5.51	4.40	1.27E-08	1.28E-08	3.58E-04	3.50E-04	1.63E-07	1.69E-07	8.78E-08	8.50E-08	3.72E-08	3.77E-08
10/28/15 0:00	4.71	3.01	1.37E-08	1.35E-08	3.61E-04	3.62E-04	1.65E-07	1.71E-07	9.25E-08	8.88E-08	3.74E-08	3.80E-08
10/28/15 4:00	4.55	1.92	1.44E-08	1.41E-08	3.75E-04	3.73E-04	1.60E-07	1.74E-07	9.09E-08	9.20E-08	3.72E-08	3.83E-08
10/28/15 8:00	4.70	3.60	1.34E-08	1.32E-08	3.54E-04	3.57E-04	1.63E-07	1.70E-07	9.10E-08	8.72E-08	3.74E-08	3.79E-08
10/28/15 11:00	6.08	3.88	1.36E-08	1.30E-08	3.38E-04	3.54E-04	1.68E-07	1.70E-07	8.90E-08	8.64E-08	3.68E-08	3.78E-08

Table 11. Noble gas data for the tufa spring

Date and Time	Water Temp (C)	Recharge Temp (C)	Xe Meas. (ccSTP/g)	Xe Theor. (ccSTP/g)	Ar Meas. (ccSTP/g)	Ar Theor. (ccSTP/g)	Ne Meas. (ccSTP/g)	Ne Theor. (ccSTP/g)	Kr Meas. (ccSTP/g)	Kr Theor. (ccSTP/g)	He4 Meas. (ccSTP/g)	He4 Theor. (ccSTP/g)
11/5/14 12:00	7.80	4.12	1.27E-08	1.28E-08	3.57E-04	3.51E-04	1.71E-07	1.71E-07	8.68E-08	8.53E-08	4.02E-08	3.84E-08
4/18/15 12:00	6.00	4.12	1.27E-08	1.29E-08	3.63E-04	3.53E-04	1.64E-07	1.70E-07	9.28E-08	8.59E-08	3.75E-08	3.79E-08
4/25/15 12:00	6.10	4.32	1.31E-08	1.28E-08	3.49E-04	3.51E-04	1.62E-07	1.69E-07	8.87E-08	8.54E-08	3.74E-08	3.78E-08
4/30/15 12:00	6.20	3.65	1.37E-08	1.32E-08	3.46E-04	3.57E-04	1.63E-07	1.71E-07	9.13E-08	8.73E-08	3.77E-08	3.80E-08
5/9/15 12:00	6.24	3.33	1.35E-08	1.33E-08	3.54E-04	3.60E-04	1.70E-07	1.71E-07	8.97E-08	8.81E-08	3.80E-08	3.80E-08
5/23/15 12:00	6.41	3.63	1.36E-08	1.32E-08	3.45E-04	3.57E-04	1.68E-07	1.71E-07	8.95E-08	8.73E-08	3.79E-08	3.80E-08
5/30/15 10:30	6.48	4.62	1.28E-08	1.27E-08	3.48E-04	3.52E-04	1.76E-07	1.76E-07	9.27E-08	8.51E-08	4.00E-08	3.98E-08
6/5/15 11:00	6.27	3.76	1.31E-08	1.31E-08	3.63E-04	3.56E-04	1.66E-07	1.70E-07	9.19E-08	8.69E-08	3.82E-08	3.79E-08
6/13/15 8:00	6.64	4.82	1.27E-08	1.26E-08	3.45E-04	3.47E-04	1.67E-07	1.68E-07	8.57E-08	8.41E-08	3.83E-08	3.77E-08
6/19/15 11:00	6.43	4.41	1.30E-08	1.28E-08	3.51E-04	3.50E-04	1.62E-07	1.69E-07	8.47E-08	8.52E-08	3.76E-08	3.78E-08
6/28/15 8:30	6.50	5.85	1.24E-08	1.21E-08	3.35E-04	3.38E-04	1.59E-07	1.66E-07	8.39E-08	8.14E-08	3.76E-08	3.75E-08
7/3/15 9:00	6.57	3.43	1.38E-08	1.33E-08	3.46E-04	3.59E-04	1.64E-07	1.71E-07	9.05E-08	8.79E-08	3.76E-08	3.80E-08
7/10/15 17:30	6.67	5.42	1.22E-08	1.23E-08	3.51E-04	3.41E-04	1.64E-07	1.67E-07	8.56E-08	8.25E-08	3.78E-08	3.76E-08
7/16/15 17:00	6.76	4.66	1.25E-08	1.27E-08	3.56E-04	3.48E-04	1.67E-07	1.69E-07	8.62E-08	8.45E-08	3.80E-08	3.77E-08
8/1/15 10:00	7.07	5.61	1.22E-08	1.22E-08	3.44E-04	3.40E-04	1.64E-07	1.67E-07	8.76E-08	8.20E-08	3.85E-08	3.75E-08
8/8/15 10:00	7.12	4.12	1.27E-08	1.29E-08	3.52E-04	3.52E-04	1.60E-07	1.69E-07	8.39E-08	8.57E-08	3.74E-08	3.78E-08
9/1/15 15:00	7.31	5.76	1.28E-08	1.22E-08	3.24E-04	3.38E-04	1.57E-07	1.67E-07	8.43E-08	8.17E-08	3.68E-08	3.75E-08
9/5/15 9:30	7.29	5.48	1.30E-08	1.23E-08	3.27E-04	3.41E-04	1.57E-07	1.67E-07	8.48E-08	8.24E-08	3.73E-08	3.76E-08

Table 11 cont.

Date and Time	Water Temp (C)	Recharge Temp (C)	Xe Meas. (ccSTP/g)	Xe Theor. (ccSTP/g)	Ar Meas. (ccSTP/g)	Ar Theor. (ccSTP/g)	Ne Meas. (ccSTP/g)	Ne Theor. (ccSTP/g)	Kr Meas. (ccSTP/g)	Kr Theor. (ccSTP/g)	He4 Meas. (ccSTP/g)	He4 Theor. (ccSTP/g)
9/12/15 7:40	7.23	5.64	1.23E-08	1.22E-08	3.39E-04	3.39E-04	1.63E-07	1.67E-07	8.27E-08	8.20E-08	3.72E-08	3.75E-08
9/19/15 7:40	7.29	5.91	1.28E-08	1.21E-08	3.19E-04	3.37E-04	1.59E-07	1.66E-07	8.61E-08	8.13E-08	3.74E-08	3.75E-08
9/27/15 9:30	7.40	4.63	1.31E-08	1.27E-08	3.34E-04	3.48E-04	1.68E-07	1.69E-07	8.51E-08	8.46E-08	3.91E-08	3.77E-08
10/2/15 7:30	7.41	4.58	1.28E-08	1.27E-08	3.54E-04	3.49E-04	1.62E-07	1.69E-07	8.40E-08	8.47E-08	3.70E-08	3.78E-08
10/9/15 7:15	7.52	5.80	1.22E-08	1.21E-08	3.37E-04	3.38E-04	1.63E-07	1.67E-07	8.78E-08	8.16E-08	3.79E-08	3.75E-08
10/15/15 16:40	7.75	4.83	1.26E-08	1.26E-08	3.49E-04	3.46E-04	1.67E-07	1.68E-07	8.72E-08	8.41E-08	3.83E-08	3.77E-08
10/27/15 8:00	7.66	5.36	1.27E-08	1.23E-08	3.37E-04	3.42E-04	1.59E-07	1.67E-07	8.24E-08	8.27E-08	3.78E-08	3.76E-08
10/27/15 12:00	7.68	7.40	1.19E-08	1.14E-08	3.13E-04	3.25E-04	1.57E-07	1.64E-07	8.09E-08	7.77E-08	3.68E-08	3.72E-08
10/27/15 16:00	7.68	6.62	1.19E-08	1.18E-08	3.37E-04	3.31E-04	1.53E-07	1.65E-07	8.65E-08	7.96E-08	3.68E-08	3.73E-08
10/28/15 0:00	7.63	4.83	1.30E-08	1.26E-08	3.33E-04	3.47E-04	1.71E-07	1.69E-07	8.36E-08	8.41E-08	3.86E-08	3.80E-08
10/28/15 4:00	7.66	6.91	1.20E-08	1.16E-08	3.16E-04	3.29E-04	1.63E-07	1.65E-07	8.42E-08	7.89E-08	3.70E-08	3.73E-08
10/28/15 8:00	7.65	5.54	1.27E-08	1.23E-08	3.31E-04	3.40E-04	1.59E-07	1.67E-07	8.23E-08	8.22E-08	3.76E-08	3.76E-08
10/28/15 11:00	7.67	3.54	1.32E-08	1.33E-08	3.72E-04	3.62E-04	1.70E-07	1.73E-07	9.13E-08	8.83E-08	3.89E-08	3.85E-08

REFERENCES

Aeschbach-Hertig, W.; Solomon, D. K. Noble Gas Thermometry in Groundwater Hydrology. In *The Noble Gases as Geochemical Tracers*; Burnard, P., Ed.; Springer Berlin Heidelberg: Berlin, Heidelberg, 2013; pp 81–122.

Aeschbach-Hertig, W.; Peeters, F.; Beyerle, U.; Kipfer, R. Palaeotemperature Reconstruction from Noble Gases in Ground Water Taking into Account Equilibration with Entrapped Air. *Nature* **2000**, *405* (6790), 1040–1044.

Bencala, K. E.; Walters, R. A. Simulation of Solute Transport in a Mountain Pool-and-Riffle Stream: A Transient Storage Model. *Water Resour. Res.* **1983**, *19* (3), 718–724.

Bencala, K. E.; Gooseff, M. N.; Kimball, B. A. Rethinking Hyporheic Flow and Transient Storage to Advance Understanding of Stream-Catchment Connections. *Water Resour. Res.* **2011**, *47* (W00H03).

Boulton, A. J.; Findlay, S.; Marmonier, P.; Stanley, E. H.; Valett, H. M. The Functional Significance of the Hyporheic Zone in Streams and Rivers. *Annu. Rev. Ecol. Syst.* **1998**, *29*, 59–81.

Canton, J. H.; Wester, P. W.; Mathijssen-Spiekman, E. A. M. Study on the Toxicity of Sodium Bromide to Different Freshwater Organisms. *Food Chem. Toxicol.* **1983**, *21* (4), 369–378.

Cook, P. G.; Lamontagne, S.; Berhane, D.; Clark, J. F. Quantifying Groundwater Discharge to Cockburn River, Southeastern Australia, Using Dissolved Gas Tracers 222Rn and SF6. *Water Resour. Res.* **2006**, *42* (W10411).

Dansgaard, W. Stable Isotopes in Precipitation. *Tellus* **1964**, *16* (4), 436–468.

Davis, S. N.; Whittemore, D. O.; Fabryka-Martin, J. Uses of Chloride/Bromide Ratios in Studies of Potable Water. *Ground Water* **1998**, *36* (2), 338–350.

Douglas, J. J.; Arbogast, T. Dual-Porosity Models for Flow in Naturally Fractured Reservoirs. In *Dynamics of Fluids in Hierarchical Porous Media*; Cushman, J. H., Ed.; Academic Press: London, 1990; pp 177–221.

Gat, J. R. Oxygen and Hydrogen Isotopes in the Hydrologic Cycle. *Annu. Rev. Earth Planet. Sci.* **1996**, *24* (1), 225–262.

Gooseff, M. N. Defining Hyporheic Zones – Advancing Our Conceptual and Operational Definitions of Where Stream Water and Groundwater Meet. *Geogr. Compass* **2010**, *4* (8), 945–955.

Gooseff, M. N. Hyporheic zone of a stream http://www.waterencyclopedia.com/St-Ts/Stream-Hyporheic-Zone-of-a.html (accessed Mar 28, 2016).

Gooseff, M. N.; Anderson, J. K.; Wondzell, S. M.; LaNier, J.; Haggerty, R. A Modelling Study of Hyporheic Exchange Pattern and the Sequence, Size, and Spacing of Stream Bedforms in Mountain Stream Networks, Oregon, USA. *Hydrol. Process.* **2006**, *20* (11), 2443–2457.

Haws, N. W.; Rao, P. S. C.; Simunek, J.; Poyer, I. C. Single-Porosity and Dual-Porosity Modeling of Water Flow and Solute Transport in Subsurface-Drained Fields Using Effective Field-Scale Parameters. *J. Hydrol.* **2005**, *313* (3–4), 257–273.

Hely, A. G.; Mower, R. W.; Harr, C. A. *Water Resources of Salt Lake County, Utah*; Utah Department of Natural Resources Technical Publication 31, 1971; Vol. DNR.

Mazor, E. Paleotemperatures and Other Hydrological Parameters Deduced from Noble Gases Dissolved in Groundwaters; Jordan Rift Valley, Israel. *Geochim. Cosmochim. Acta* **1972**, *36* (12), 1321–1336.

Mazor, E. *Chemical and Isotopic Groundwater Hydrology: The Applied Approach*, 2nd ed.; Halsted Press: New York, 1997.

McGuire, K. J.; McDonnell, J. J. A Review and Evaluation of Catchment Transit Time Modeling. *J. Hydrol.* **2006**, *330* (3–4), 543–563.

Ogata, A.; Banks, R. B. *A Solution of the Differential Equation of Longitudinal Dispersion in Porous Media*; Professional Paper No. 411-A 411–A; U.S. Geological Survey, 1961.

Solomon, D. K. Dissolved and Noble Gases http://www.noblegaslab.utah.edu/dissolved_gas.html (accessed Feb 26, 2016).

Stolp, B. Determining Mean Transit Times of Groundwater Flow Systems. Ph.D. Dissertation, University of Utah: Salt Lake City, UT, 2014.

Zimmerman, R. W.; Chen, G.; Bodvarsson, G. S. A Dual-Porosity Reservoir Model with an Improved Coupling Term; Stanford, CA, 1992.

SAHRA - Isotopes & Hydrology http://web.sahra.arizona.edu/programs/isotopes/oxygen.html (accessed Jul 18, 2016).